Biogeosciences, 22, 975–994, 2025
https://doi.org/10.5194/bg-22-975-2025

Biogeosciences Open Access EGU

Climate-driven shifts in Southern Ocean primary producers and biogeochemistry in CMIP6 models

Ben J. Fisher[1,a], **Alex J. Poulton**[2], **Michael P. Meredith**[3], **Kimberlee Baldry**[4], **Oscar Schofield**[5], **and Sian F. Henley**[1]

[1]School of GeoSciences, University of Edinburgh, Edinburgh, United Kingdom
[2]The Lyell Centre for Earth and Marine Sciences and Technology, Heriot-Watt University, Edinburgh, United Kingdom
[3]British Antarctic Survey, Cambridge, United Kingdom
[4]Institute for Marine and Antarctic Studies, College of Sciences and Engineering, University of Tasmania, Hobart, TAS, Australia
[5]Center for Ocean Observing Leadership, School of Environmental and Biological Sciences, Rutgers University, New Brunswick, NJ 08901, USA
[a]now at: The Lyell Centre for Earth and Marine Sciences and Technology, Heriot-Watt University, Edinburgh, United Kingdom

Correspondence: Ben J. Fisher (b.fisher@hw.ac.uk)

Received: 1 April 2024 – Discussion started: 26 April 2024
Revised: 16 December 2024 – Accepted: 17 December 2024 – Published: 20 February 2025

Abstract. As a net source of nutrients fuelling global primary production, changes in Southern Ocean productivity are expected to influence biological carbon storage across the global ocean. Following a high-emission, low-mitigation pathway (SSP5-8.5), we show that primary productivity in the Antarctic zone of the Southern Ocean is predicted to increase by up to 30 % over the 21st century. The ecophysiological response of marine phytoplankton experiencing climate change will be a key determinant in understanding the impact of Southern Ocean productivity shifts on the carbon cycle. Yet, phytoplankton ecophysiology is poorly represented in Coupled Model Intercomparison Project phase 6 (CMIP6) climate models, leading to substantial uncertainty in the representation of its role in carbon sequestration. Here we synthesise the existing spatial and temporal projections of Southern Ocean productivity from CMIP6 models, separated by phytoplankton functional type, and identify key processes where greater observational data coverage can help to improve future model performance. We find substantial variability between models in projections of light concentration ($>15\,000$ ($\mu E\,m^{-2}\,s^{-1}$)^2) across much of the iron- and light-limited Antarctic zone. Projections of iron and light limitation of phytoplankton vary by up to 10 % across latitudinal zones, while the greatest increases in productivity occurs close to the coast. Temperature, pH and nutrients are less spatially variable – projections for 2090–2100 under SSP5-8.5 show zonally averaged changes of $+1.6$ °C and -0.45 pH units and Si* ($[Si(OH)_4]$–$[NO_3^-]$) decreases by 8.5 µmol L^{-1}. Diatoms and picophytoplankton and/or miscellaneous phytoplankton are equally responsible for driving productivity increases across the subantarctic and transitional zones, but picophytoplankton and miscellaneous phytoplankton increase at a greater rate than diatoms in the Antarctic zone. Despite the variability in productivity with different phytoplankton types, we show that the most complex models disagree on the ecological mechanisms behind these productivity changes. We propose that a sampling approach targeting the regions with the greatest rates of climate-driven change in ocean biogeochemistry and community assemblages would help to resolve the empirical principles underlying the phytoplankton community structure in the Southern Ocean.

1 Introduction

The biological uptake of carbon by marine phytoplankton represents an important process in the Earth system (Deppeler and Davidson, 2017), with ocean carbon storage mediating atmospheric CO_2 concentrations, including CO_2 of anthropogenic origin (Riebesell et al., 2007). Across the global

ocean, uptake of carbon accounts for ∼ 25 % of CO_2 released by human activities (Friedlingstein et al., 2022). The Southern Ocean is a disproportionately large carbon and heat sink relative to its size (Frölicher et al., 2015), accounting for 30 %–40 % of this global anthropogenic CO_2 uptake (e.g. Caldeira and Duffy, 2000; DeVries, 2014), predominantly due to enhanced atmosphere–ocean exchange at increased atmospheric CO_2 concentrations (Friedlingstein et al., 2022). While biological uptake is considered to play a minor role in total CO_2 uptake (Landschutzer et al., 2015; Gruber et al., 2019), variability in pCO_2 has been associated with summertime blooms in the Southern Ocean (Gregor et al., 2018; Coggins et al., 2023). Under a future climate scenario with longer growth seasons (Moreau et al., 2015), increased seasonal productivity (Leung et al., 2015; Fu et al., 2016) and a reduction in ocean CO_2 absorption efficiency (higher Revelle factor) (Hauck et al., 2015), biological and physical drivers of carbon exchange across the air–sea interface are likely to undergo substantial changes. As the ocean's buffering capacity for increasing concentrations of atmospheric CO_2 reduces (Jiang et al., 2019), the role of pelagic ecosystems is expected to become increasingly important in Southern Ocean carbon uptake (Henley et al., 2020).

Small-celled marine phytoplankton (0.002–0.2 mm) are responsible for the production of biological carbon which fuels ecosystems but are vulnerable to environmental change because of their specific requirements for light and iron, which are the primary factors limiting their growth in high-nutrient low-chlorophyll (HNLC) zones of the Southern Ocean (Moore et al., 2013). Following a "middle of the road" SSP2-4.5 pathway, being the scenario which most closely represents the current climate trajectory, between 2015 and 2023, Southern Ocean phytoplankton (defined as those south of 30° S following Gregg et al., 2003) represented 36.31 % of marine net primary productivity globally, equivalent to 15.5 Pg C yr^{-1} (Fig. S1). Climate impacts on Southern Ocean phytoplankton are likely to manifest as ecological shifts towards smaller cell sizes (Venables et al., 2013; Saba et al., 2014; Schofield et al., 2018; Biggs et al., 2019; Mascioni et al., 2019) and changes in seasonal phenology (Moreau et al., 2015). Increases in overall productivity can be most closely associated with a reduced duration and extent of sea ice coverage, allowing for a greater supply of irradiance to surface waters of this light and iron co-limited productivity system. This increase in ocean surface area available for light transmission is offset by decreased insolation (−8.3 %, Fig. 1) associated with a greater degree of cloud cover. Strengthened upwelling is also likely to increase the flux of existing iron supplies to the coastal (Annett et al., 2015) and open ocean (Moreau et al., 2023) from sedimentary or hydrothermal sources; however, the extent to which changes in ocean mixing can be expected to impact nutrient supplies remains largely unknown (Fig. 1).

Shifts in community composition from diatoms to smaller cryptophytes have already been documented along the west Antarctic Peninsula (Moline et al., 2004; Ducklow et al., 2007; Moline et al., 2008; Montes-Hugo et al., 2008; Rozema et al., 2017) and are thought to be due to tolerance of cryptophytes to the low-salinity waters induced by increased sea ice melt (Moline et al., 2004) or the tolerance of cryptophytes for high- and variable-light conditions in well-stratified surface layers (Mendes et al., 2023). Conversely, in culture-based competition experiments, diatoms are more successful in simulated future ocean conditions than prevalent haptophytes such as *Phaeocystis antarctica*, albeit with reduced diatom cell sizes (Xu et al., 2014). This difference is potentially driven by reduced iron limitation of diatoms and their greater tolerance to temperature change (Zhu et al., 2016). These varied responses between manipulation experiments and in situ observations suggest that both physiological and ecological adaptations are important for understanding the net biogeochemical implications of phytoplankton community change.

In the sea ice zone, grazing by zooplankton accounts for ∼ 90 % of phytoplankton losses (Moreau et al., 2020). Shifts in phytoplankton size class could rapidly cascade through the ecosystem as the dominant Southern Ocean zooplankton, Antarctic krill (*Euphausia superba*, hereafter krill), are unable to graze small cryptophytes (Haberman et al., 2003). Instead, this promotes the growth of carbon-poor salps (*Salpa thompsoni*), which reduces the overall efficiency of the marine food web (Ballerini et al., 2014) and potentially weakens the biological carbon pump (Quéguiner, 2013; Biggs et al., 2021). Additionally, water temperature, alongside changes to zooplankton abundance and diversity, has been shown to increase zooplankton metabolism (Lopez-Urrutia et al., 2006; Mayzaud and Pakhomov, 2014), which can in turn be expected to modulate the grazing pressure and phytoplankton biomass (Lewandowska et al., 2014). Due to the strong relationship between temperature and metabolism in zooplankton, their abundance has been observed to follow the fronts of the Southern Ocean, with poleward contractions in salp and krill populations in response to warming (Constable et al., 2014; Atkinson et al., 2019).

Projections of productivity in the Southern Ocean under future climate scenarios from the Coupled Model Intercomparison Project phase 6 (CMIP6) class Earth system models (ESMs) are actively informing research directions, Intergovernmental Panel on Climate Change (IPCC) reports (Masson-Delmotte et al., 2021) and governmental policy (Touzé-Peiffer et al., 2020). Yet, between CMIP5 and CMIP6, the spread of model projections with respect to vertical and horizontal physics and the number of phytoplankton functional types included have increased as different models incorporate more complexity and additional processes (e.g. varying elemental stoichiometry, phytoplankton diversity, complex elemental cycling) (Seferian et al., 2020). While representation of ocean physical drivers and nutrient fields compared to observations has improved between CMIP5 and CMIP6, surface chlorophyll is one of three key

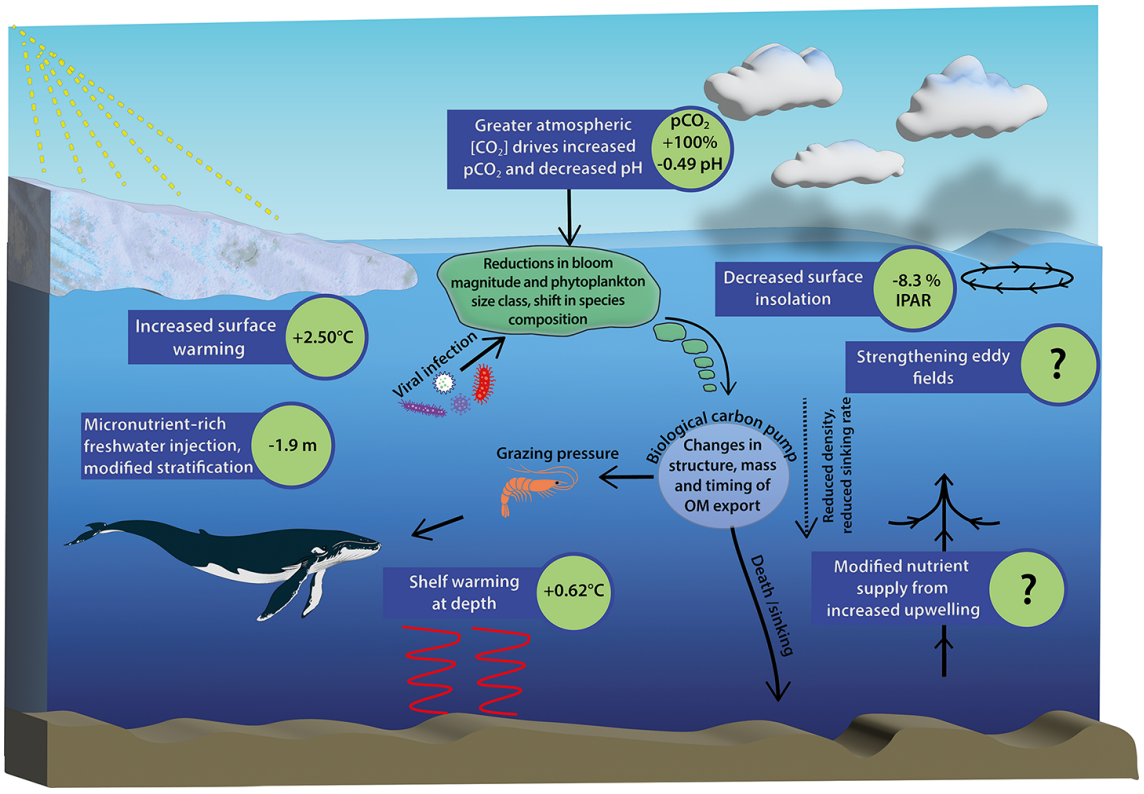

Figure 1. Schematic diagram of Southern Ocean pressures associated with climate change and the downstream biogeochemical consequences for ecosystem productivity. Values shown for surface warming, surface insolation and pH are 100-year mean changes to 2100 under the SSP5-8.5 scenario south of 65° S and are taken from Coupled Model Intercomparison Project phase 6 (CMIP6) models. Literature values are used for changes in pCO_2, stratification and shelf warming at depth for the same time period and climate trajectory (Kawaguchi et al., 2013; Hauck et al., 2015; Purich and England, 2021) (see Table S1 for a full description). Question marks indicate key processes which drive biogeochemical change but are not currently included in CMIP models, and therefore estimations of change do not currently exist.

parameters that did not show improvement in benchmarking of CMIP6 performance over the global ocean (Canadell et al., 2021; Fu et al., 2022). Variance in model projections of phytoplankton and ocean biogeochemistry has been linked to the use of fixed C : N : P elemental stoichiometry (Kwiatkowski et al., 2018); an inability to reflect physiological adaptations, e.g. the ability of diatoms to maintain growth under iron limitation (Person et al., 2018); and complexities in modelling export fluxes (Henson et al., 2022), particularly in constraining phytoplankton losses through zooplankton grazing (Cavan et al., 2017).

A major difference in the representation of productivity between CMIP6 models is the extent to which they consider different classes of phytoplankton. Diatoms (>20 µm) and pico-/nanophytoplankton (predominantly cryptophytes and haptophytes) represent the vast majority of productivity across all latitudes of the Southern Ocean. Diatoms are a significant contributor to primary production and carbon export, accounting for ∼40 % of global marine primary production and particulate organic carbon (POC) exported to depth in the ocean (Jin et al., 2006; Tréguer et al., 2017). Diazotrophs (nitrogen-fixing phytoplankton) are present in small numbers, usually only in subtropical niches, due to the excess supply of nitrogen across the Southern Ocean (Luo et al., 2012). Calcifiers, mostly coccolithophores, inhabit waters north of 60° S where there is a strong supply of light but low-Si, high-Fe conditions, preventing the growth of diatoms (Charalampopoulou et al., 2016; Nissen et al., 2018). Only three CMIP6 models specifically include diatoms and picophytoplankton under future warming conditions (CESM2, CESM2-WACCM and GFDL-ESM4).

In recent years, record-low sea ice concentrations have been observed in the Southern Ocean (Raphael and Handcock, 2022; Turner et al., 2022). Given the dependence of Southern Ocean productivity on the timing of seasonal sea ice retreat, we consider it possible that this shift in trends of sea ice concentration could cause an abrupt change to sea-ice-dependent ecosystems in the near future (Swadling et al., 2023). This is proposed to manifest in reduced algal, copepod, krill and fish populations with subsequent negative impacts on birds, mammals and associated ecosystem services (Steiner et al., 2021). As phytoplankton are the main source of organic carbon in the Southern Ocean, uncertainty in projections of phytoplankton composition compounds existing

model uncertainty in the biological carbon flux to the ocean's interior and seafloor (Henson et al., 2022). Within the context of climate change in the Southern Ocean, reducing model uncertainty in ecosystem-mediated biogeochemical cycling will be of increased importance in determining the global-scale impact of changes in the Southern Ocean productivity regime.

In this study we aim to

1. quantify the degree of uncertainty between models in projections of phytoplankton productivity with an SSP5-8.5 warming scenario, including different phytoplankton functional types;

2. determine mean trends between projected climate-driven change in ecosystems, physical processes and biogeochemical cycling across different latitudinal zones of the Southern Ocean;

3. identify regions, time frames and processes within the Southern Ocean Observing System (SOOS) framework (https://soos.aq, last access: 19 December 2024), where the greatest projected changes and/or uncertainties occur.

2 Methods

Model and observational data for the Southern Ocean were collected and visualised to determine (a) the physical and biogeochemical changes that force or result from shifts in productivity and (b) the extent of primary productivity shifts over the next century in CMIP6.

2.1 CMIP projections

Model output was obtained from the Coupled Model Intercomparison Project phase 6 (CMIP6) data server via https://pangeo.io (last access: 19 December 2024) using the xmip package in Python 3.11. Ensemble members for each parameter were chosen based on their availability for historical *(hist)* and SSP5-8.5 *(ssp585)* (ScenarioMIP) data (O'Neill et al., 2016). The selected models for each parameter are detailed in Table 1. Where an analysis type relied on the direct comparison between two or more parameters, only models that contained both parameters were selected. For the analysis presented in Sect. 3.5, annual net primary production (*intpp*) is only included from models which also include the diatom-specific annual net primary production (*intppdiat*) parameter. Where the same baseline model is included twice, because of having a low- and high-resolution version, the model is pre-averaged (i.e. both resolutions are assigned a weighting of 0.5 each) to avoid double counting of the same model when calculating the ensemble mean. Examples of models with two resolutions are highlighted in bold in Table 1. Only a small number of CMIP6 models contain irradiance limitation (*limirr*) and iron limitation (*limfe*) for multiple phytoplankton types; therefore analyses of light and iron limitation of phytoplankton utilise <5 models. All variables were extracted at monthly frequency, except for surface wind speeds where data were initially obtained daily; subsequently, annual weighted means were generated for most parameters following the weighting algorithm by Grover (2021). For mixed-layer depth and incidental photosynthetically active radiation (IPAR), austral summertime means were used instead of annual means.

Model data were processed in Python 3.11 to apply the desired analysis (e.g. annual average, annual maximum) and then further averaged over residual variables (e.g. member_id). In most cases, all available member_id's were used; where this was not possible, any member_id's which could not be aggregated due to differences in array structure were removed. Net primary production (NPP) is provided as a pre-integrated value across the water column; we integrated chlorophyll across the depth dimension between 0 and 500 m to capture all phytoplankton across different depths, using the integrate function in SciPy (Virtanen et al., 2020). Subsequently, all models were re-gridded to a rectilinear grid via bilinear or nearest-neighbour interpolation using XESMF (Zhuang et al., 2018) before being averaged to create multi-model means.

For spatial plotting, data were projected onto the Antarctic Polar Stereographic (EPSG:3031) coordinate reference system in ArcGIS Pro and visualised in QGIS using the Quantarctica package (Matsuoka et al., 2021), with postprocessing using SAGA and GDAL tools to remove imperfections in grid alignment through interpolation. All code to extract the CMIP6 data used in this study is available open access.

2.2 Regional data

Historical sea surface temperature and concentrations of surface nitrate and silicic acid were mapped from the World Ocean Atlas 2018 data product (Garcia et al., 2019), representing average values from 1955 to 2017. For Si*, annually averaged data for nitrate and silicic acid were exported at a $1 \times 1^{\circ}$ resolution and subtracted from one another to produce Si*. Commonly observed marine variables (chlorophyll, temperature, nutrients, pH) were analysed by their regional sector using the Southern Ocean Observing System (SOOS) framework. The purpose of integrating CMIP6 projections within the main existing observation framework is to identify regions of the largest expected changes in routinely observed variables to inform the coordination of future sampling efforts by the SOOS regional working groups. Additionally, SOOS regions provide an additional quantification of heterogeneity in marine variables within the latitudinal zones. To determine Si*, pH and temperature values by SOOS area, SOOS regions south of 55° were drawn as mask layers and subset using the zonal statistics function in QGIS.

Table 1. Selected models used in analysis of CMIP6 data based on availability in the Pangeo Catalog. Models shown in bold represent multiple resolutions of the same core model, which were subsequently averaged prior to calculation of the ensemble mean. Where direct comparisons are made between multiple parameters, ensembles were adjusted to include only models which existed for all of the selected parameters.

Variable ID	Parameter	Units	Data selection	Models selected
intpp	Primary organic carbon production by all types of phytoplankton/diatoms	$gC\,m^{-2}\,yr^{-1}$	Annual average	ACCESS-ESM1-5, CanESM5, CanESM5-CanOE, CESM2, CESM2-WACCM, CMCC-ESM2, CNRM-ESM2-1, EC-Earth3-CC, GFDL-ESM4, GFDL-CM4, IPSL-CM6A-LR, MIROC-ES2L, **MPI-ESM1-2-HR, MPI-ESM1-2-LR**, MRI-ESM2-0, **NorESM2-LM, NorESM2-MM**, UKESM1-0-LL
intppdiat				CanESM5-CanOE, CESM2-WACCM, CNRM-ESM2-1, GFDL-ESM4, IPSL-CM6A-LR, UKESM1-0-LL
chl	Mass concentration of total phytoplankton expressed as chlorophyll in seawater	$kg\,m^{-3}$	Annual average	ACCESS-ESM1-5, CanESM5, CanESM5-CanOE, CESM2, CESM2-WACCM, CMCC-ESM2, GFDL-CM4, GFDL-ESM4, MIROC-ES2L, **MPI-ESM1-2-HR**, **MPI-ESM1-2-LR**, MRI-ESM2-0, **NorESM2-LM**, **NorESM2-MM**, UKESM1-0-LL
limirrpico	Irradiance limitation of picophytoplankton/ miscellaneous phytoplankton/diatoms/diazotrophs	Ratio of growth under environmental irradiance to growth under unlimited irradiance	Annual average	CESM2-WACCM, GFDL-ESM4
limirrmisc				CanESM5, CNRM-ESM2-1,GFDL-ESM4, IPSL-CM6A-LR
limirrdiat				CESM2-WACCM, CNRM-ESM2-1, GFDL-ESM4, IPSL-CM6A-LR, UKESM1-0-LL
limirrdiaz				CESM2-WACCM, GFDL-ESM4
limfediat/pico/misc	Iron limitation of diatoms/picophytoplankton/miscellaneous phytoplankton	Ratio of growth under environmental iron concentration to growth under unlimited iron concentration	Combined annual average	GFDL-ESM4
rsntds	Net downward shortwave radiation at seawater surface (IPAR)	$W\,m^{-2}$ (converted to $\mu E\,m^{-2}\,s^{-1}$)	Summertime (daily) maximum	ACCESS-CM2, CanESM5, CanESM5-CanOE, CESM2-WACCM, CMCC-CM2-SR5, **CNRM-CM6-1**, **CNRM-CM6-1-HR**, CNRM-ESM2-1, EC-Earth3, EC-Earth3-CC, EC-Earth3-Veg, IPSL-CM6A-LR, MIROC-ES2L, **MPI-ESM1-2-HR**, **MPI-ESM1-2-LR**, **NorESM2-LM**, **NorESM2-MM**
sfcWindmax	Daily maximum near-surface wind speed	$m\,s^{-1}$	Annual average of daily maxima	AWI-CM-1-1-MR, BCC-CSM2-MR, CanESM5, CMCC-CM2-SR5, CMCC-ESM2, **CNRM-CM6-1**, **CNRM-CM6-1-HR**, CNRM-ESM2-1, EC-Earth3, EC-Earth3-CC, **EC-Earth3-Veg**, **EC-Earth3-Veg-LR**, GFDL-CM4, HadGEM3-GC31-MM, INM-CM4-8, INM-CM5-0, IPSL-CM6A-LR, KACE-1-0-G, **MPI-ESM1-2-HR**. **MPI-ESM1-2-LR**, MRI-ESM2-0, UKESM1-0-LL
mlotst	Ocean mixed-layer thickness defined by σ_t	m	Summertime maximum	ACCESS-CM2, BCC-CSM2-MR, CAMS-CSM1-0, CanESM5, CanESM5-CanOE, CESM2, CESM2-WACCM, CNRM-CM6-1, CNRM-ESM2-1, GFDL-ESM4, GISS-E2-1-G, HadGEM3-GC31-LL, IPSL-CM6A-LR, MPI-ESM1-2-HR, MRI-ESM2-0, NESM3, UKESM1-0-LL
phos	Sea surface pH	pH units	Annual average	CanESM5, CanESM5-CanOE, CESM2, CESM2-WACCM, GFDL-ESM4, IPSL-CM6A-LR, MIROC-ES2L, MRI-ESM2-0, NorESM2-LM
tos	Sea surface temperature	°C	Annual average	ACCESS-CM2, ACCESS-ESM1-5, BCC-CSM2-MR, CAMS-CSM1-0, CanESM5, CanESM5-CanOE, CESM2, CESM2-WACCM, CIESM, CMCC-CM2-SR5, CMCC-ESM2, **CNRM-CM6-1**, **CNRM-CM6-1-HR**, CNRM-ESM2-1, E3SM-1-1, EC-Earth3, EC-Earth3-CC, **EC-Earth3-Veg**, **EC-Earth3-Veg-LR**, FGOALS-f3-L, FGOALS-g3, FIO-ESM-2-0, GFDL-CM4, GFDL-ESM4, **HadGEM3-GC31-LL**, **HadGEM3-GC31-MM**, IITM-ESM, INM-CM4-8, INM-CM5-0, IPSL-CM6A-LR, KACE-1-0-G, KIOST-ESM, MCM-UA-1-0, MIROC6, MIROC-ES2L, **MPI-ESM1-2-HR**, **MPI-ESM1-2-LR**, MRI-ESM2-0, NESM3, **NorESM2-LM**, **NorESM2-MM**, TaiESM1, UKESM1-0-LL

Table 1. Continued.

Variable ID	Parameter	Units	Data selection	Models selected
sios	Surface concentration of silicic acid	$\mu mol\,L^{-1}$	Annual average	CanESM5-CanOE, GFDL-ESM4, IPSL-CM6A-LR, **MPI-ESM1-2-HR**, **MPI-ESM1-2-LR**, **NorESM2-LM**, **NorESM2-MM**, UKESM1-0-LL
no3os	Surface concentration of nitrate	$\mu mol\,L^{-1}$	Annual average	CESM2, CESM2-WACCM, GFDL-ESM4, NorESM2-LM, UKESM1-0-LL
limno3	Nitrate limitation of phytoplankton	Ratio of growth under environmental nitrate concentration to growth under unlimited nitrate concentration	Annual average	GFDL-ESM4

3 Results and discussion

3.1 Physical climate drives biological changes in Southern Ocean water masses

Climate change is driving substantial changes in Southern Ocean water masses (Bindoff et al., 2019). The widespread strengthening of Southern Ocean winds by up to $0.8\,m\,s^{-1}$ (Fig. 2a) and increased buoyancy fluxes (including freshwater inputs) act as opposing drivers of stratification, modifying mixed-layer depth (Fig. 2b). Mixed layers are projected to deepen across the subantarctic by up to 10 m but shoal across much of the rest of the Southern Ocean (Fig. 2b). In light-limited regions, a shoaling of the mixed layer can be expected to increase productivity, as phytoplankton become concentrated closer to the surface, while in iron-limited regions, where iron is supplied by wintertime vertical mixing, deeper mixed layers can benefit depth-integrated primary productivity by increasing the productive water volume over which iron concentrations are sufficient to promote growth (Llort et al., 2019). Subsequently, the changing availability of light and iron across the Southern Ocean determines the abundance and composition of primary producers. Despite the importance of changes in Southern Ocean circulation for global ocean nutrient supply, the cumulative influence of physical processes across different spatial resolutions results in poor overall performance of CMIP class models in this region when their historical runs are compared with observations (Meredith et al., 2019). A particular weakness of CMIP6 models is in reconstructing the sea ice changes that drive buoyancy forcing (Roach et al., 2020; Shu et al., 2020), which has an important role in determining the flux of heat and CO_2 across the ocean–atmosphere boundary. The uncertainty in sea ice change also results in a high degree of variation in coastal irradiance between models (Fig. S2e), particularly for the Weddell Sea and Ross Sea regions. Recent large and unexpected changes in sea ice around Antarctica emphasise that greater knowledge of the key drivers and controls is required in order to improve predictive skill in models (Turner and Comiso, 2017).

Across the Southern Ocean, the timing of the springtime onset of net primary production and the magnitude of summer biomass accumulation are controlled by light availability, as dictated by sea ice extent, cloud cover and water column structure (Henley et al., 2017). CMIP6 models project the greatest relative increase in productivity to occur across the Antarctic zone of the Southern Ocean (65–90° S) (Figs. 2c, S3), where irradiance limitation is reduced (Fig. 2d). Conversely, across the transitional zone (40–50° S), IPAR reduces (Fig. 2e) with cloud cover, driving changes in light beyond the sea ice zone; irradiance limitation increases (Fig. 2d); and relative productivity increases are smaller here compared to the coastal Southern Ocean (Figs. 2c, S3). Increased iron limitation (Fig. 2f) likely manifests from greater competition for iron driven by increased productivity (Fig. 2c). This is despite a potential increase in iron supply with a deepening of the mixed layer across parts of the subantarctic (50–65° S) (Fig. 2b), brought about by reduced upper-ocean stratification from strengthening zonal winds (Carranza and Gille, 2015; Sallee et al., 2021). Increased iron limitation across much of the Antarctic and subantarctic coincides with reduced light limitation (Fig. 2d) beyond the region where IPAR increases (Fig. 2e); this is consistent with greater iron demand from increased productivity (Fig. 2c), driving phytoplankton to iron limitation before light limitation. Iron supply to the surface is subject to changes in the properties and movement of water masses, which lead to variable circulation strengths, depth boundaries, heat content and carbon sequestration, resulting from climate-driven perturbations to the ice–ocean–atmosphere system (Bindoff et al., 2019; Meredith et al., 2019). Upwelling of nutrients and light availability for phytoplankton are both strongly influenced by mixed-layer depth, which in turn varies seasonally with increased solar warming and ice melt, driving deeper Southern Ocean pycnocline stratification through the summer (Sallee et al., 2021). Models generally agree on changes in summertime mixed-layer depth across most of the open ocean (Fig. S2b) – the greatest source of uncertainty is at the terminus of the Ross (Ross Sea) and Flichner–Ronne (Weddell Sea) ice shelves. This uncertainty in stratification can be linked to the lack of representation of ice shelves and

their meltwater flux in the current generation of CMIP models (Purich and England, 2021). Subsequently, the lack of a meltwater flux directly impacts biology and biogeochemical cycles through the absence of ice-associated nutrient seeding (e.g. Death et al., 2014) alongside creating uncertainty in nutrient and light availability through an incomplete representation of stratification.

3.2 Changing biogeochemistry of the Southern Ocean

3.2.1 Micronutrient supply and uptake

Iron acts as the primary limiting nutrient across the Southern Ocean (de Baar et al., 1995; Watson et al., 2000) due to supply limitation from low-atmospheric inputs and significant distances from terrigenous sources (Boyd and Ellwood, 2010). Around the Antarctic coast, iron concentrations are set by processes including the resuspension of shelf sediments (Blain et al., 2001) and melting of sea ice (Lannuzel et al., 2016). The change in projected iron limitation of phytoplankton appears minimal (between $-12\,\%$ and $+10\,\%$, Fig. 2f). Iron limitation is expected to increase most in the transitional zone between South America and Aotearoa / New Zealand, correlating with a reduction in near-surface wind speed (Fig. 2a), suggesting that atmospheric deposition of iron could decline in this region. There is a minor increase in iron limitation around the Antarctic coast, which represents the inverse of the decreasing trend in irradiance limitation (Fig. 2d), indicating a shift towards an increasingly iron-limited system, as reductions in sea ice concentrations increase light availability to coastal waters. The co-occurrence of an increase in iron limitation (Fig. 2f) and an increase in total productivity (Fig. 2c) across the Antarctic zone suggests that this increase in limitation is driven by an increase in the uptake of iron (from a larger productivity sink), as opposed to any substantial changes in supply.

Despite the importance of iron for phytoplankton growth in the Southern Ocean, CMIP series models have struggled to resolve the vertical supply of dissolved iron (Tagliabue et al., 2016), resulting in uncertainty in modelling primary and export productivity. At the group level, iron limitation could be expected to influence shifts in phytoplankton communities because larger cells may have a greater demand for iron compared to smaller cells (Hudson and Morel, 1990; Timmermans et al., 2004). In addition, other micronutrients, such as manganese, have been identified as a control on phytoplankton growth, particularly during seasonal transitions (Pausch et al., 2019; Browning et al., 2021; Balaguer et al., 2022), yet only iron is considered in ESMs due to, at least partially, the lack of observational data to underpin distribution modelling of other micronutrients. Future work should continue to develop our understanding of the metabolic role of other micronutrients and additionally consider the extent to which diversity exists in micronutrient demand among Southern Ocean phytoplankton species.

3.2.2 Macronutrient supply and uptake

Nitrogen species, silicic acid (DSi) and phosphate are all essential for the growth and survival of diatoms, with nitrate and phosphate also being required by all other phytoplankton classes for cellular metabolism. Unlike much of the global ocean (Moore et al., 2013), high rates of macronutrient supply from the Circumpolar Deep Water (CDW) prevent widespread N or P limitation in the Southern Ocean, except in periods of intense summer growth in high-productivity coastal regions (Henley et al., 2017). Although projections indicate an increase in chlorophyll across such regions (Fig. 3), models do not show any substantial increases in nitrate limitation south of the subtropical zone over the remainder of the century (Fig. S4), suggesting that iron and light will continue to be the primary constraints on productivity.

While macronutrients are not usually limiting to Southern Ocean phytoplankton, growth of diatom communities, particularly around high-productivity coastal and island zones (supported by lateral iron advection) (Robinson et al., 2016), is likely to place an increased demand on DSi availability (Table 2). The relationship between Si and N is denoted as Si* (Sarmiento et al., 2004), with high Si* values (>25) indicating plentiful DSi availability that supports diatom growth, while low values (<10) suggest conditions which favour non-silicifying phytoplankton, such as the smaller cryptophytes and haptophytes. Si* is the highest in the Antarctic zone (Henley et al., 2020) because of silica input from upwelling of CDW but remains spatially heterogeneous within this region (Table 2). Si* is consistently high in the Weddell Sea, while across the West Antarctic Peninsula (WAP) and Ross, Amundsen and Bellingshausen seas, there is a moderate mean Si* with large variability, and the Indian sector has a substantially lower DSi availability. Si* is projected to decline by 2090–2100 at a zonally averaged value of $-8.5\,\mu mol\,L^{-1}$, with the greatest declines being in the Ross and Weddell seas, as well as the Indian sector (Table 2).

Decreases in Si* coincide with increases in chlorophyll concentration across the same regions (Fig. 3), concurring with increased phytoplankton concentrations, resulting in a drawdown of silicic acid. However, increases in chlorophyll appear independently of projected changes in primary productivity (Fig. 2c). For example, the west Antarctic Peninsula and Amundsen Sea regions show the greatest increase in primary productivity but are among the regions with the smallest change for both Si* and chlorophyll. The divergence between chlorophyll and primary productivity indicates variability in Chl : C, with siliceous diatoms typically expressing more chlorophyll per unit of carbon (Sathyendranath et al., 2009). Therefore, the large chlorophyll increases and large Si* decline projected in the Weddell Sea are driven by an increase in diatoms (Fig. S5), whereas the productivity increases with only small changes in both chlorophyll and Si* seen on the west Antarctic Peninsula result from an

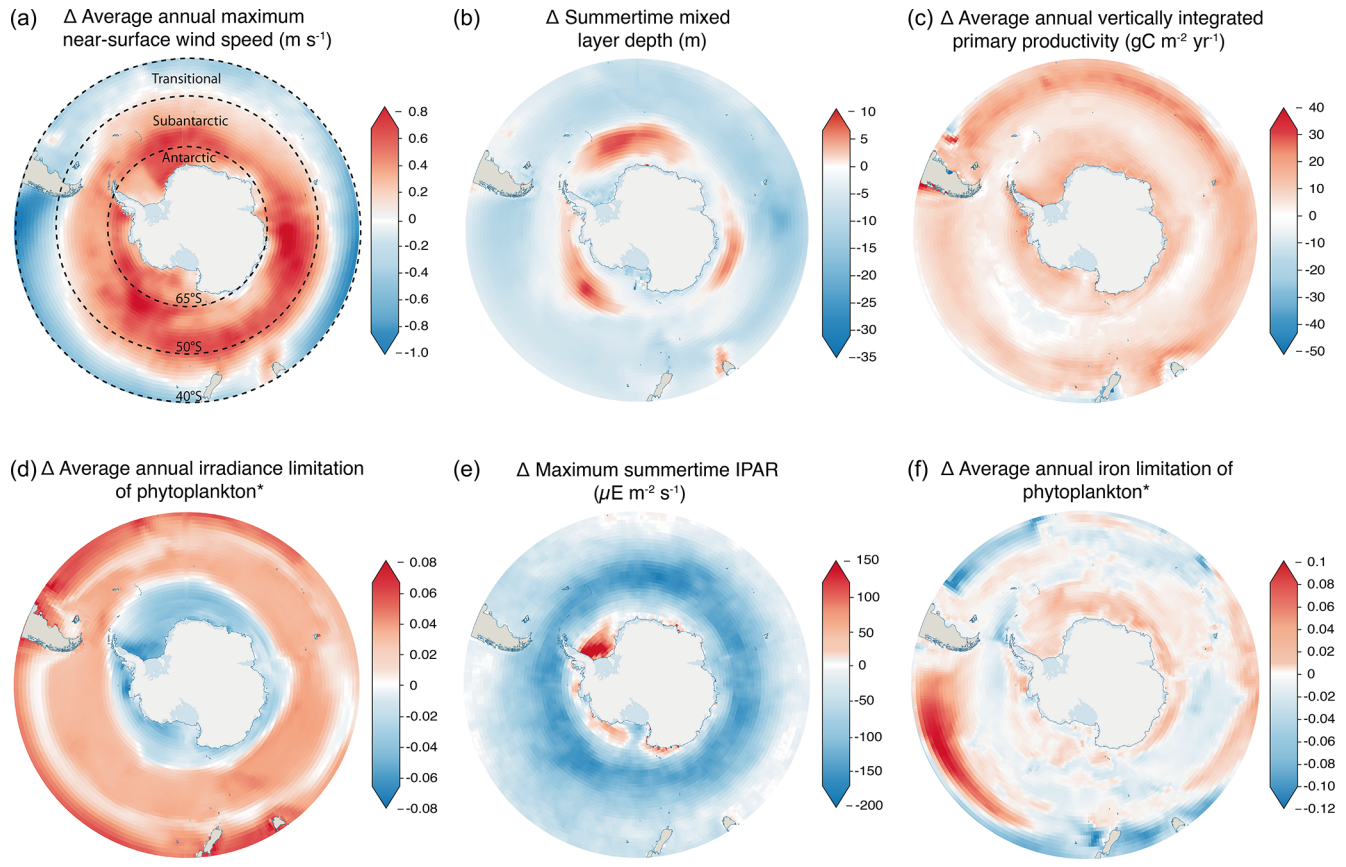

Figure 2. CMIP6 anomaly representing change at the end of the century in **(a)** near-surface wind speed, **(b)** mixed-layer depth, **(c)** net primary productivity, **(d)** irradiance limitation of phytoplankton, **(e)** incidental photosynthetically active radiation (IPAR) and **(f)** iron limitation of phytoplankton. Changes are calculated from an ensemble of CMIP6 models, comparing a historical (1985–2015) average against 2090–2100 under the SSP5-8.5 climate scenario. Details of ensemble members are given in Table 1. Units in panels **(d)** and **(f)** (the panels with the asterisks) are arbitrary ratios of growth under environmental irradiance or iron concentrations to potential growth under unlimited irradiance or iron concentrations. Positive values represent an increase in limitation, while negative values represent a decrease in limitation. Latitudinal contours are shown for Fig. 2a; these represent the northern boundaries of the Antarctic, subtropical and transitional zones.

expansion of non-diatom phytoplankton with lower Chl : C (Fig. S6).

The impact of climate change on DSi supply to the surface is difficult to evaluate because it is dependent on the competing stratification effects from wind-driven changes to upwelling and an increase in freshening. Export of DSi from the surface and remineralisation at depth additionally act as important controls on supply; Freeman et al. (2018) showed that increased biological uptake of silicic acid, through increased diatom growth, leads to a poleward shift in the silicic acid front and a potential decoupling from the Antarctic polar front. Efforts to better define the nutrient budgets, particularly in increasingly common low-sea-ice years, across different sectors of the Southern Ocean and understand the changing nutrient demands of phytoplankton will be essential for determining future trends in nutrient limitation (Henley et al., 2019).

3.2.3 Ocean acidification

Across all regions of the Southern Ocean, continued uptake of anthropogenic CO_2 is expected to elicit a decrease in surface pH of $\sim$0.45 units south of 55° S (Table 2) under the high-emission scenario (SSP5-8.5). Projected changes in pH do not differ regionally and show little variation within regions (low standard deviation); therefore regional changes in phytoplankton growth do not result from a direct acidification effect. In the CMIP6 models, phytoplankton growth is usually driven and limited by nutrients and light, and while many models are built with complex carbonate systems, these typically only interact with rates of calcification, and for the majority of phytoplankton there is no biotic feedback from changes to the carbonate system. This lack of biotic feedback prevents ocean acidification (OA) from impacting the main biological members of the Southern Ocean in CMIP6 despite expected acidification effects on diatom (Petrou et al., 2019), picophytoplankton (Tortell

et al., 2008) and krill (Kawaguchi et al., 2013) populations. A more complex representation of phytoplankton acidification effects in CMIP6 should include the interactive effect of acidification on phytoplankton stoichiometry, e.g. reduced silicification (Si : C) of diatoms (Petrou et al., 2019). This change would allow OA to influence carbon export via modifying silicification, in addition to the existing modelled controls on phytoplankton silica content set by silicic acid and iron concentrations (Moore et al., 2004; Stock et al., 2014). Expanding model setups in CMIP6 to include the impact of OA and other physiochemical drivers on biogeochemical stoichiometry could help to resolve existing biases in Southern Ocean silicic acid concentrations (Long et al., 2021).

3.3 Primary production and representation in CMIP6

Two CMIP6 models (GFDL-ESM4 and CESM2-WACCM) showed substantial mechanistic differences in productivity projections by phytoplankton type south of 65° S (Fig. 4). While GFDL-ESM4 projects that in this region diatoms account for the majority (60 %) of the change in productivity under SSP5-8.5 (Fig. 4a, b), diatoms represent only 28 % of the productivity increase in CESM2-WACCM, with picophytoplankton forming the major (72 %) phytoplankton group (Fig. 4e, d). Additionally, the GFDL model indicates that increased productivity is driven by increases in both diatoms and picophytoplankton, representing a simultaneous growth scenario, while CESM2-WACCM favours a replacement mechanism with diatoms decreasing as picophytoplankton populations grow (Fig. 4c, f). In CESM2-WACCM (MARBL biogeochemistry module) and GFDL-ESM4 (COBALTv2 biogeochemistry module), growth of phytoplankton groups is a product of temperature, nutrient limitation and light availability. In COBALTv2 the iron uptake half-saturation constant is greater than in MARBL (0.1 vs. 0.03 nmol kg^{-1} for small phytoplankton), and the differential between small and large phytoplankton (diatom) iron requirements is greater (×5 vs. ×2.3). Although phytoplankton in MARBL have lower Fe requirements, negative biases towards NO_3^- and PO_4^{-3} in the Southern Ocean by CESM2 suggest that net community productivity is overestimated; subsequently this could drive the system to iron limitation earlier, resulting in an "insufficient contribution from diatoms" (Long et al., 2021). This could suggest that GFDL-ESM4 presents a more realistic outlook on phytoplankton composition; however fixed nutrient constants, which usually represent a global average collected from multiple studies, make no differentiation for changes to nutrient uptake in cold-water environments. For example, Timmermans et al. (2004) showed that iron uptake half-saturation values for Southern Ocean diatoms varied substantially between 0.19 and 1.14 nmol L^{-1} for different diatom species compared to a fixed value of 0.5 nmol L^{-1} for COBALTv2 and 0.07 for MARBL, representing diatoms globally (Stock et al., 2020; Long et al., 2021). Experimentally, uptake half-saturation constants are determined through the sequential addition of nutrients, yet multiple studies have shown that Southern Ocean diatoms in particular are able to reduce their cellular iron demand through changes to the photosynthetic pathway (e.g. Strzepek and Harrison, 2004; Jabre et al., 2021). Therefore, models based on these fixed constants may be reflecting the maximal iron uptake rather than the low-iron-acclimated uptake; i.e. this approach towards modelling nutrient limitation does not allow for a molecular adaptation, which can, in some cases, achieve the same growth rate under more limiting conditions.

A shift from single species to community-based phytoplankton experiments for the purpose of biogeochemical rates would help to improve our understanding of variability within the broad groups that exist for describing phytoplankton in CMIP6 models. For example, dynamic nutrient acquisition rates for different types of diatoms could replace a fixed nutrient half-saturation constant for all diatom species if sufficient datasets existed to describe such rates at the species level. Developments of marine ecosystem models may include an expanded range of biological interactions, such as group-specific phytoplankton–zooplankton predation and bacterially driven mixotrophic effects, and such processes could alter trophic energy transfer and export fluxes through ESMs (Ward and Follows, 2016). Trait-based approaches have been explored as a means of modelling phytoplankton community composition, distinguishing functional groups based on life histories, morphology and physiology (Litchman and Klausmeier, 2008). Ocean biological sampling has some of the lowest coverage in the Southern Ocean (Sunagawa et al., 2020). Expansion of ecosystem observing at the metagenomics level (e.g. Guidi et al., 2016) offers a promising opportunity to expand our knowledge of traits and trade-offs in Southern Ocean phytoplankton communities, facilitating their integration into climate models.

In a changing ocean, phytoplankton will succeed where they have the greatest biological plasticity, for example the ability to photo-acclimate rapidly (Arrigo et al., 2010) or utilise a diverse range of nutrients (Kwon et al., 2022). The physiological properties of any individual species ultimately determine their ability to survive in a particular region at a particular time under ever-changing climate-driven conditions. Subsequently, species ecology determines the abundance and temporal extent with which a species can exist or compete in a particular region. As warming continues to bring about an earlier retreat of sea ice, growth seasons are expected to lengthen, altering the temporal dynamics of species progression (Moreau et al., 2015). In the Antarctic zone of the Southern Ocean, changes in light appear to be the main influence on productivity, with decreased irradiance limitation stimulating picophytoplankton growth to a greater extent than diatoms (Fig. 4j, k, m, n); meanwhile iron limitation shows little correlation with productivity changes in this region, with an R^2 of 0.51 for picophytoplankton and

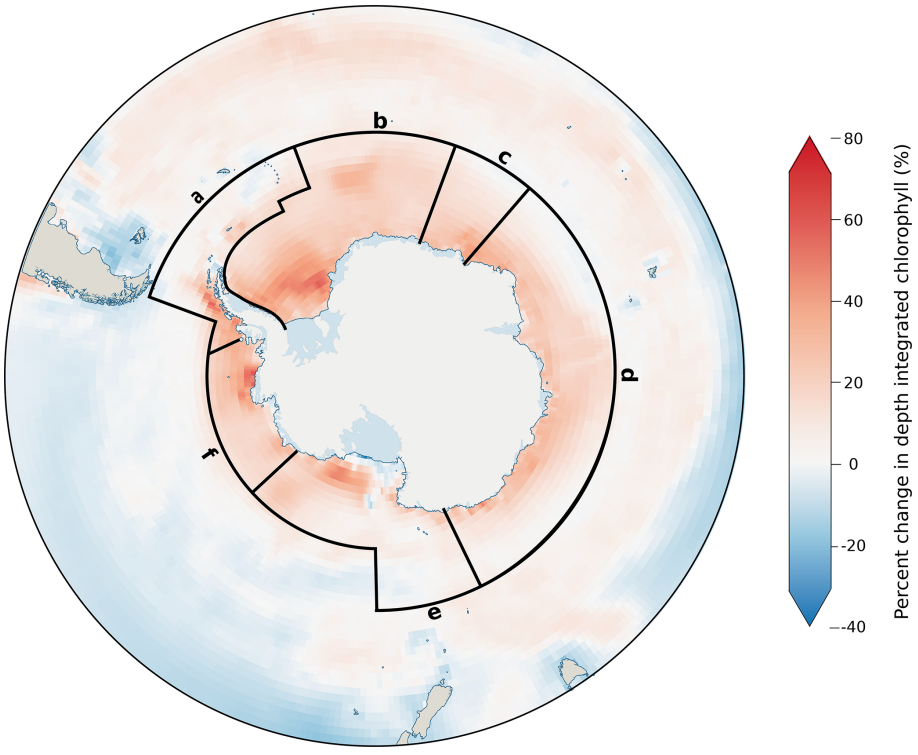

Figure 3. Change in depth-integrated chlorophyll (0–500 m) from all phytoplankton, displayed as the percentage change between the annual historical average (1985–2015) and projected values for 2090–2100. Values shown are multi-model means of the models listed in Table 1. Spatial boundaries show the Southern Ocean Observing System (SOOS) regions south of 55° S, which are defined in Table 2.

Table 2. Biogeochemical parameter values calculated for the Southern Ocean Observing System regions. SOOS regional working groups (as defined at https://www.soos.aq/activities/rwg, last access: 11 February 2025) are indicated in Fig. 3; section C is an overlap section of sections B and D. Data shown are Si* ($[Si(OH)_4]$–$[NO_3^-]$) values and temperature determined from objectively analysed annual means of World Ocean Atlas 2018 data. pH was determined from a historical run of a multi-model ensemble of CMIP6 models (1985–2015). Delta values are anomalies of multi-model means of pH, temperature and Si* based on comparisons between the mean annual historical value (1985–2015) and projected values for 2090–2100 under SSP5-8.5 for a CMIP6 ensemble (detailed in Table 1). Values in brackets are standard deviations, representing spatial variation across the region. Anomaly maps for pH, temperature and Si* are shown in Figs. S7, S8 and S9 respectively.

Section	SOOS region	Si* ($\mu mol\,L^{-1}$)	ΔSi* ($\mu mol\,L^{-1}$)	pH	Δ pH	Temperature (°C)	Δ Temperature (°C)
A	West Antarctic Peninsula and Scotia Arc	17.24 (17.82)	−7.06 (3.63)	8.07 (0.15)	−0.43 (0.01)	1.94 (1.87)	1.79 (0.37)
B	Weddell Sea and Dronning Maud Land (WSDML)	37.37 (9.70)	−10.98 (3.77)	8.08 (0.14)	−0.41 (0.01)	−0.07 (0.95)	1.43 (0.49)
C	Southern Ocean Indian Sector (SOIS)/WSDML	23.16 (6.67)	−8.20 (1.59)	8.07 (0.01)	−0.41 (0.01)	1.08 (1.26)	1.89 (0.40)
D	SOIS (3.72)	4.71 (3.67)	−10.52 (0.13)	8.07 (0.01)	−0.41 (1.66)	1.78 (0.46)	1.78
E	Ross Sea	19.82 (18.49)	−9.13 (5.02)	8.08 (0.13)	−0.40 (0.02)	0.62 (2.22)	1.08 (0.46)
F	Amundsen and Bellingshausen seas	17.59 (14.02)	−5.27 (4.33)	8.09 (0.16)	−0.43 (0.01)	0.11 (0.83)	1.73 (0.44)

0.06 for diatoms (Fig. 4g, h), likely because of replete iron supplies from coastal upwelling.

3.4 Latitudinal productivity projections in CMIP6

From the models that do distinguish between at least diatoms and other phytoplankton, we are able to examine projected changes in community composition over the 21st century under a continued warming scenario (SSP5-8.5) (Fig. 5). Previous analysis by Laufkötter et al. (2015), using a different set of models (a mix of marine ecosystem models employed in CMIP5 and the Marine Ecosystem Model Intercomparison Project), found substantial disagreement between models in projecting which phytoplankton groups drove NPP changes in the Southern Ocean. In CMIP5, Leung et al. (2015) found a latitudinally banded response of phytoplankton to continued warming, driven by the bottom-up dynamics of nitrate, iron and light limitation. From this analysis, we applied the same latitudinal bands to our analysis of the changes in whole-community, diatom and non-diatom productivity across CMIP6. Our whole-community projections agree with the trends shown by Leung et al. (2015) of a poleward increase in phytoplankton productivity, increasing average total productivity south of 40° S, with increases in total productivity in the transitional (40–50° S; Fig. 5b), subantarctic (50–60° S; Fig. 5c) and Antarctic zones (65–90° S; Fig. 5d). In relative terms, this reflects a $\sim 10\,\%$ increase in total productivity over the SSP5-8.5 run (2015–2100) for both the transitional and the subantarctic zones, with a $\sim 30\,\%$ increase in productivity for the Antarctic zone (Fig. S10b, c, d). The poleward increases in productivity correlate with a deepening of mixed layers around the Antarctic zone (Fig. 2b) and a reduction in coastal light limitation (Fig. 2d), resulting in greater increases in Antarctic zone productivity compared to the transitional or subantarctic. An ensemble mean shows no overall change in productivity across the subtropics (see also Tagliabue et al., 2021); however individual models show the widest degree of divergence in this region, with some models projecting decreases in the diatom population of over 60 % (Fig. S10a), indicating a large uncertainty in the magnitude of productivity changes. Compositional changes in primary productivity across the subtropics are driven by reductions in nutrient availability from increased stratification (Fu et al., 2016), as reflected in the increase in nitrate limitation across these regions (Fig. S4). Under nutrient stress, smaller phytoplankton can outperform larger phytoplankton, here diatoms, because of lower nutrient demands, leading to the modelled declines in diatom populations (Fig. 7). The divergence in nutrient half-saturation constants between different models (see Sect. 3.3) subsequently leads to a wide range of projections in species composition when nutrients become limiting.

In the subantarctic (50–65° S), despite a large projected increase in light availability (Fig. 2e), models project only a minor increase in productivity driven by a small amount of diatom growth, suggesting that growth of both diatom and non-diatom species remains largely iron-limited in this region. The Antarctic zone shows the greatest degree of change in phytoplankton growth, with the largest increases in this region. The majority of the biomass change can be attributed to non-diatoms; however relative changes in both diatom and non-diatom populations are similar (Fig. S10d), suggesting no overall changes to community composition here. The continued increase in all phytoplankton classes can be attributed to the decreased iron limitation across much of the zone (Fig. 2f), with the success of non-diatoms reflecting the increase in light limitation (Fig. 2d). Large phytoplankton types are more strongly affected by light limitation in CMIP6 because they have a greater requirement for light (as a lower constant for the chlorophyll-specific initial slope of the photosynthesis–irradiance curve); in COBALTv2, large phytoplankton require 3 times as much light as small phytoplankton to reach the same rate of photosynthesis (Stock et al., 2020). The lower requirements for iron and light of smaller phytoplankton types mean that the change in relative abundance of smaller phytoplankton types in response to environmental change is often greater compared to diatom populations.

While CMIP6 models do not explicitly consider phytoplankton size, the shift from diatoms to typically smaller, non-diatom species is consistent with more advanced ecological models, such as DARWIN, which predict a decrease in the slope of the phytoplankton size spectrum, albeit over a greater area of the Southern Ocean than shown in CMIP6 (Henson et al., 2021). Despite the clear differences between latitudinal bands, spatial heterogeneity continues to exist within these zones, particularly for the Antarctic zone where some of the greatest increases in chlorophyll occur in the WAP and Weddell Sea regions (Fig. 3), reflecting the disproportionately high DSi supply in these regions (Table 2). Resolving spatial heterogeneity in phytoplankton in global-scale models such as those in CMIP6 is likely to require an increased reliance on, and integration with, regional-scale modelling (Person et al., 2018). The rapid increase in non-diatom species around the coast is in agreement with studies describing declining large diatom ($>20\,\mu m$) abundances (Kang et al., 2001; Wright et al., 2010; Pearce et al., 2011); however, while it is true that diatoms are projected to decrease as a proportion of the community, diatom-derived carbon production is still projected to increase under continued warming, suggesting that the coastal biological carbon pump may be less threatened by this shift in community composition than previously thought.

4 Conclusions

4.1 Implications of Southern Ocean productivity shifts

The cumulative impact of climate change on phytoplankton has the potential to restructure ecosystems of the Southern

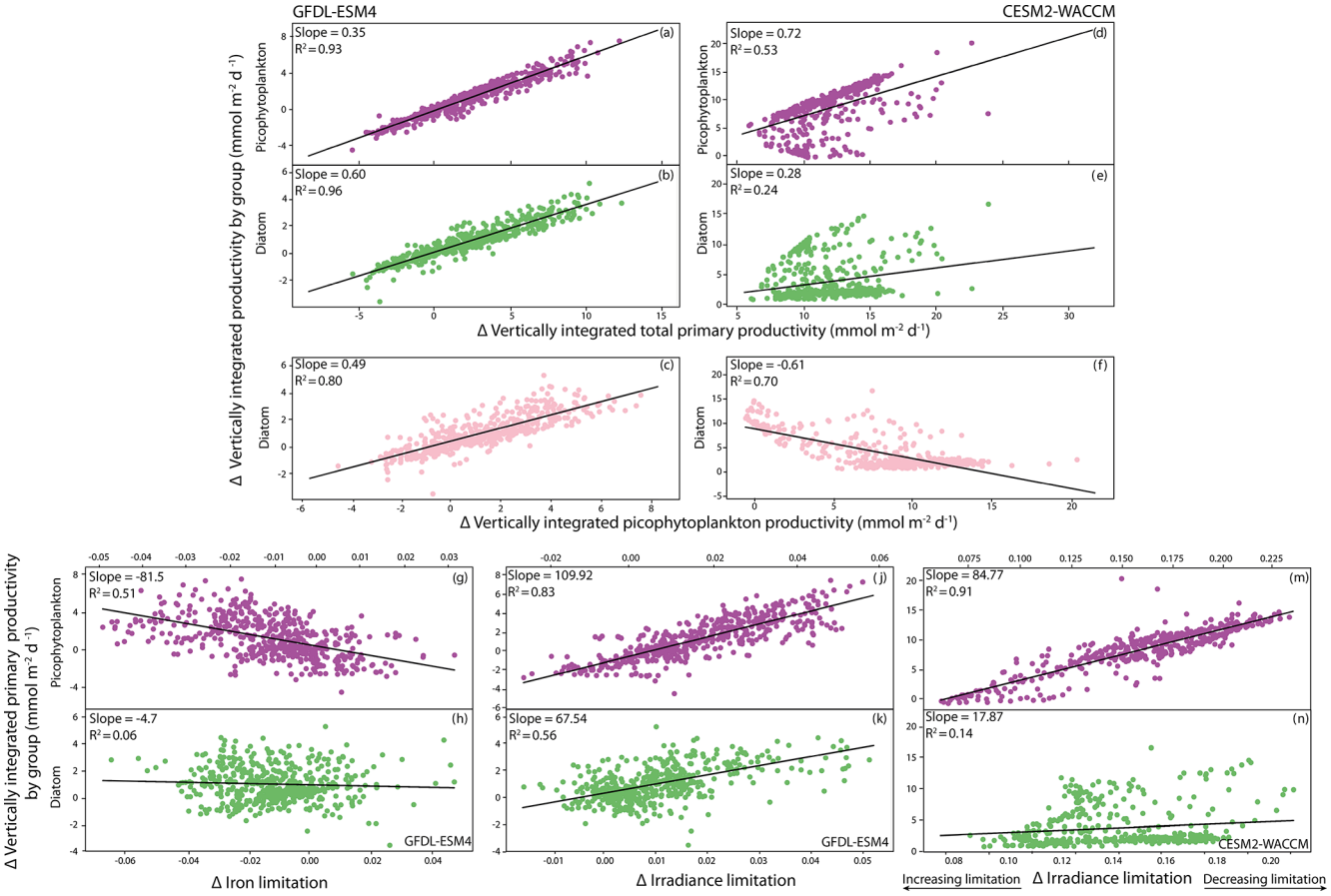

Figure 4. Evaluation of GFDL-ESM4 and CESM2-WACCM models using an anomaly between 2090–2100 (SSP5-8.5) and a historical average (1985–2015) for the Antarctic zone (65–90° S). Linear regression between change in total productivity and picophytoplankton productivity for GFDL-ESM4 **(a)** and CESM2-WACCM **(d)**. Linear regression between change in total productivity and diatom productivity for GFDL-ESM4 **(b)** and CESM2-WACCM **(e)**. Linear regression between change in picophytoplankton productivity and diatom productivity for GFDL-ESM4 **(c)** and CESM2-WACCM **(f)**. Change in iron limitation with picophytoplankton **(g)** and diatom **(h)** productivity for GFDL-ESM4. Change in irradiance limitation with picophytoplankton **(j)** and diatom **(k)** productivity for GFDL-ESM4. Change in irradiance limitation with picophytoplankton **(m)** and diatom **(n)** productivity for CESM2-WACCM.

Ocean, with wider consequences for global ocean productivity and climate. In this study we found that CMIP6 models project a future Southern Ocean with increased levels of productivity, particularly around the Antarctic coastal zone. The major driver of this is reductions in light limitation, brought about by increased light concentrations from reduced sea ice coverage. However, the extent to which light will change is a source of great uncertainty, with the poor performance of sea ice in CMIP6 also having additional implications for buoyancy forcing. Resolving freshwater fluxes from the Antarctic Ice Sheet could reduce model uncertainty in coastal mixed-layer depth change. The current iteration of CMIP6 models does not suggest any significant shifts in the average community composition between latitudinal bands across the Southern Ocean, outside of a decrease in the relative abundance of diatoms in the subtropical zone. However, there is a large uncertainty of up to ±30 % for all phytoplankton classes across all zones of the Southern Ocean (Fig. S10), and key processes which will impact phytoplankton (e.g. viral losses, composition of the grazer community) are absent from most models. A lack of complexity in the representation of zooplankton communities accounts for a large degree of uncertainty in phytoplankton composition and the marine carbon cycle (Rohr et al., 2023); this is particularly acute for the Southern Ocean where the major zooplankton fractions, salps and krill, feed on distinctly different size fractions of phytoplankton. However, Heneghan et al. (2023) find that within the context of climate change, uncertainty in Southern Ocean phytoplankton distributions in a warmer ocean leads to uncertainty in future zooplankton projections. Improving the predictive skill of CMIP6 models for Southern Ocean phytoplankton could therefore unlock mutual benefits for increasing the accuracy of zooplankton model outputs.

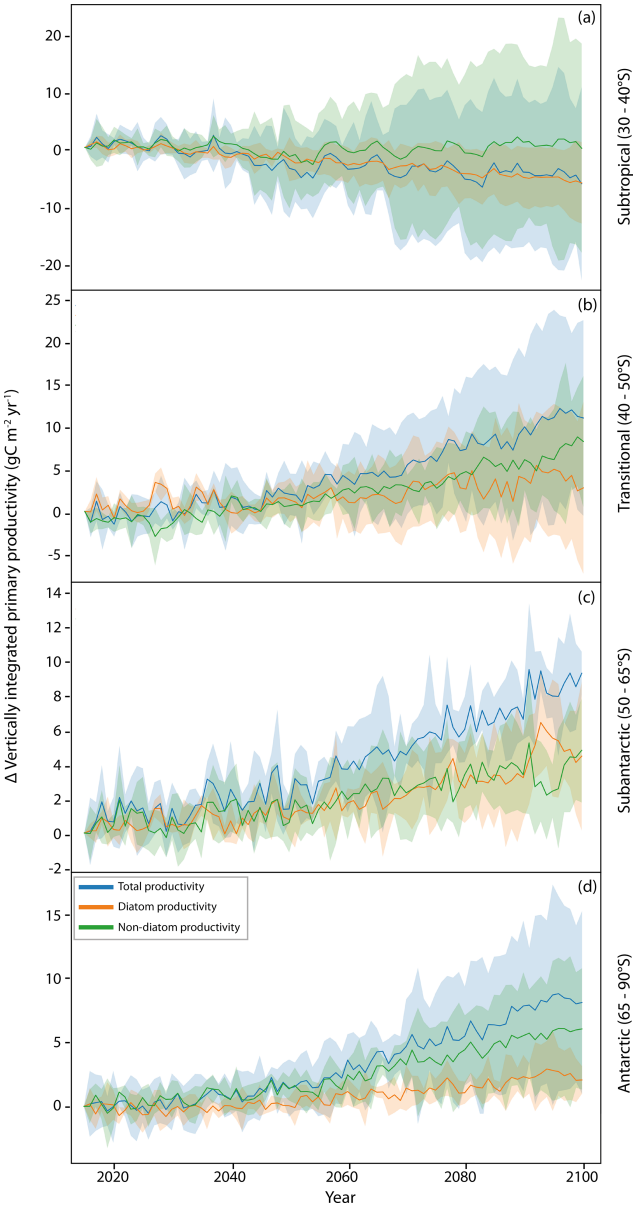

Figure 5. Changes in productivity ($g\,C\,m^{-2}\,yr^{-1}$) and the contribution of different phytoplankton classes to productivity, 2015–2100. The anomaly in CMIP6 model productivity projections (as POC production) compared to 2015 for SSP5-8.5 conditions spatially averaged across four latitudinal bands of the Southern Ocean, following Leung et al. (2015). The lines represent the multi-model means of total productivity (intpp), diatom productivity (intppdiat) and non-diatom productivity (intpp-intppdiat). The shaded regions represent the spread between models as the interquartile range. Six CMIP6 models were used in this analysis because only models containing the diatom productivity parameter are included; details of the specific models assessed are given in Table 1.

In models which do separate productivity by phytoplankton type, the growth of one type of phytoplankton over another is a product of light, temperature and nutrient limitation. Fixed nutrient stoichiometry is a key limitation in projecting phytoplankton composition; in particular, the lack of interaction between physiochemical processes such as OA with biogeochemistry could be responsible for some of the existing biases in models towards excess Si in the Southern Ocean. We showed that for two models (GFDL-ESM4 and CESM2-WACCM) the iron requirements of different phytoplankton types can result in either a simultaneous growth of diatoms and picophytoplankton or a replacement of diatoms with picophytoplankton. Future model generations might consider the acclimation of diatoms to low-iron conditions, as models currently use very different uptake half-saturation values for iron, which disproportionally impacts community composition in iron-limited regions. However, the literature also contains wide divergence in experimentally determined nutrient uptake constants (see Sect. 3.3). A more accurate approach towards modelling will first require us to better define what drives this variability in iron requirements. With continued record-low sea ice trends, observation of phytoplankton responses in this multi-stressor environment will be essential for understanding the scale of productivity change occurring and will provide a basis to incorporate phytoplankton community change into global-scale modelling efforts.

4.2 Observational recommendations

Opportunities to improve the representation of Southern Ocean biogeochemical processes in CMIP encountered in this paper can be grouped into three approaches: (a) adding currently unrepresented physical processes, (b) increasing the complexity of existing biological processes and (c) updating values used as constants in existing model processes to reflect regional variability (e.g. nutrient half-saturation constants specific to the Southern Ocean). Observational monitoring is crucial for developing the evidence required to improve the representation of temporal (e.g. nutrient fluxes from AIS melt), spatial (e.g. biogeochemical impacts of eddies) and biological (e.g. integrating size-specific metrics for zooplankton rates, traits and stocks; Ratnarajah et al., 2023) variability for incorporation into models. Within this resource-limited environment, this study sought to identify regions with the largest expected changes and uncertainties in biogeochemically linked parameters as targets for future observational work. By monitoring change across these suggested target regions, we can (a) supplement existing datasets to reduce the range of uncertainties and (b) use areas of extreme projected change as test beds for mechanistic studies to identify critical thresholds and tipping points in biogeochemical relationships.

For phytoplankton groups, the largest degree of uncertainty is in the abundance of diatoms and non-diatoms between 40 and 65° S. This is particularly acute for diatom

abundance across the transitional zone where the scale of uncertainty spans positive and negative values for most of the present century. Within the models, spatial variability in transitional zone diatom populations correlates with changes to nitrate limitation. Areas of the transitional zone which are close to land also account for the largest uncertainties in model ensemble projections of primary productivity ($>1000\,\mathrm{g\,C\,m^2\,yr^{-1}}$). The concentration of nitrate across the lower latitudes in regions close to land should be a key priority for observation as this will inform our understanding of the viability of diatom populations in the lower latitudes and reduce the $\sim 60\,\%$ uncertainty in the modelled poleward movement of diatom communities towards the subantarctic under climate change. Across the subantarctic, the largest increases in diatom populations are projected to occur over the SOOS Southern Ocean Indian Sector (SOIS), a region which is poorly studied relative to the WAP and Weddell and Ross seas. Improving the coverage of phytoplankton community composition studies in the SOIS could be most fruitful in observing the movement of diatoms between latitudinal zones. Meanwhile, the largest relative change in productivity ($>200\,\%$) is expected to occur across the Weddell Sea, which could make the Weddell Sea an increasingly important observational target for the mechanistic study of wider ecosystems, including zooplankton grazing patterns on different phytoplankton types. From the identification of these trends in the CMIP6 model ensembles, we propose that model projections could be used to target our observational capacity towards regions where enhanced data collection would be most beneficial in reducing uncertainties and ground-truthing expected rates of change. Consequently, this would strategically increase our evidence base to fill data and process knowledge gaps and inform future generations of ESM projections, improving our ability to project and observe biogeochemical change across the Southern Ocean in response to climate change.

Data availability. The CMIP6 data included in this study are available online (https://esgf-node.llnl.gov/search/cmip6/, ESGF, 2025). Specific models and parameters extracted for each analysis are listed in Table 1. Code for CMIP6 data analysis is available at https://doi.org/10.5281/zenodo.14536775 (Fisher et al., 2024).

Supplement. The supplement related to this article is available online at https://doi.org/10.5194/bg-22-975-2025-supplement.

Author contributions. BJF, SFH, MPM and AJP devised the concept for the paper and contributed towards writing the initial draft and editing. BJF performed model analysis and produced the figures. OS and KB provided input on conceptual design and edited previous versions of the manuscript. All authors have approved the final version of the paper.

Competing interests. The contact author has declared that none of the authors has any competing interests.

Disclaimer. Publisher's note: Copernicus Publications remains neutral with regard to jurisdictional claims made in the text, published maps, institutional affiliations, or any other geographical representation in this paper. While Copernicus Publications makes every effort to include appropriate place names, the final responsibility lies with the authors.

Acknowledgements. Ben J. Fisher is supported by a NERC Doctoral Training Partnership grant (NE/S007407/1). Sian F. Henley would like to acknowledge support from NERC (NE/K010034/1). This work used JASMIN, the UK's collaborative data analysis environment (https://jasmin.ac.uk, last access: 19 December 2024). We acknowledge the World Climate Research Programme, which, through its Working Group on Coupled Modelling, coordinated and promoted CMIP6. We thank the climate modelling groups for producing and making available their model output, the Earth System Grid Federation (ESGF) for archiving the data and providing access, and the multiple funding agencies who support CMIP6 and ESGF.

Financial support. This research has been supported by the Natural Environment Research Council (grant nos. NE/S007407/1 and NE/K010034/1).

Review statement. This paper was edited by Tina Treude and reviewed by two anonymous referees.

References

Annett, A. L., Skiba, M., Henley, S. F., Venables, H. J., Meredith, M. P., Statham, P. J., and Ganeshram, R. S.: Comparative roles of upwelling and glacial iron sources in Ryder Bay, coastal western Antarctic Peninsula, Mar. Chem., 176, 21–33, https://doi.org/10.1016/j.marchem.2015.06.017, 2015.

Arrigo, K. R., Mills, M. M., Kropuenske, L. R., van Dijken, G. L., Alderkamp, A. C., and Robinson, D. H.: Photophysiology in two major southern ocean phytoplankton taxa: photosynthesis and growth of Phaeocystis antarctica and Fragilariopsis cylindrus under different irradiance levels, Integr. Comp. Biol., 50, 950–966, https://doi.org/10.1093/icb/icq021, 2010.

Atkinson, A., Hill, S. L., Pakhomov, E. A., Siegel, V., Reiss, C. S., Loeb, V. J., Steinberg, D. K., Schmidt, K., Tarling, G. A., and Gerrish, L.: Krill (Euphausia superba) distribution contracts southward during rapid regional warming, Nat. Clim. Change, 9, 142–147, 2019.

Balaguer, J., Koch, F., Hassler, C., and Trimborn, S.: Iron and manganese co-limit the growth of two phytoplankton groups dominant at two locations of the Drake Passage, Commun. Biol., 5, 207, https://doi.org/10.1038/s42003-022-03148-8, 2022.

Ballerini, T., Hofmann, E. E., Ainley, D. G., Daly, K., Marrari, M., Ribic, C. A., Smith, W. O., and Steele, J. H.: Productivity and linkages of the food web of the southern region of the western Antarctic Peninsula continental shelf, Prog. Oceanogr., 122, 10–29, https://doi.org/10.1016/j.pocean.2013.11.007, 2014.

Biggs, T. E. G., Alvarez-Fernandez, S., Evans, C., Mojica, K. D. A., Rozema, P. D., Venables, H. J., Pond, D. W., and Brussaard, C. P. D.: Antarctic phytoplankton community composition and size structure: importance of ice type and temperature as regulatory factors, Polar Biol., 42, 1997–2015, https://doi.org/10.1007/s00300-019-02576-3, 2019.

Biggs, T. E. G., Huisman, J., and Brussaard, C. P. D.: Viral lysis modifies seasonal phytoplankton dynamics and carbon flow in the Southern Ocean, ISME J., 15, 3615–3622, https://doi.org/10.1038/s41396-021-01033-6, 2021.

Bindoff, N. L., Cheung, W. W., Kairo, J. G., Arístegui, J., Guinder, V. A., Hallberg, R., Hilmi, N. J. M., Jiao, N., Karim, M. S., and Levin, L.: Changing ocean, marine ecosystems, and dependent communities, IPCC special report on the ocean and cryosphere in a changing climate, 477–587, https://www.ipcc.ch/site/assets/uploads/sites/3/2019/11/09_SROCC_Ch05_FINAL-1.pdf (last access: 11 February 2025), 2019.

Blain, S., Tréguer, P., Belviso, S., Bucciarelli, E., Denis, M., Desabre, S., Fiala, M., Jézéquel, V. M., Le Fèvre, J., Mayzaud, P., Marty, J. C., and Razouls, S.: A biogeochemical study of the island mass effect in the context of the iron hypothesis:: Kerguelen Islands, Southern Ocean, Deep-Sea Res. Pt. I, 48, 163–187, https://doi.org/10.1016/S0967-0637(00)00047-9, 2001.

Boyd, P. W. and Ellwood, M. J.: The biogeochemical cycle of iron in the ocean, Nat. Geosci., 3, 675–682, https://doi.org/10.1038/ngeo964, 2010.

Browning, T. J., Achterberg, E. P., Engel, A., and Mawji, E.: Manganese co-limitation of phytoplankton growth and major nutrient drawdown in the Southern Ocean, Nat. Commun., 12, 884, https://doi.org/10.1038/s41467-021-21122-6, 2021.

Caldeira, K. and Duffy, P. B.: The role of the southern ocean in uptake and storage of anthropogenic carbon dioxide, Science, 287, 620–622, https://doi.org/10.1126/science.287.5453.620, 2000.

Canadell, J. G., Monteiro, P. M., Costa, M. H., Da Cunha, L. C., Cox, P. M., Alexey, V., Henson, S., Ishii, M., Jaccard, S., Koven, C., Lohila, A., Patra, P. K., Piao, S., Rogelj, J., Syampungani, S., Zaehle, S., and Zickfield, K.: Global carbon and other Biogeochemical Cycles and Feedbacks, in: Climate Change 2021: The Physical Science Basis. Contribution of Working Group I to the Sixth Assessment Report of the Intergovernmental Panel on Climate Change edited by: Masson-Delmotte, V., Zhai, P., Pirani, A., Connors, S. L., Péan, C., Berger, S., Caud, N., Chen, Y., Goldfarb, L., Gomis,M. I., Huang, M., Leitzell, K., Lonnoy, E., Matthews, J. B. R., Maycock, T. K., Waterfield, T., Yelekçi, O., Yu, R., and Zhou, B., Cambridge University Press, in press, https://doi.org/10.1017/9781009157896.007, 2021.

Carranza, M. M. and Gille, S. T.: Southern Ocean wind-driven entrainment enhances satellite chlorophyll-*a* through the summer, J. Geophys. Res.-Oceans, 120, 304–323, https://doi.org/10.1002/2014jc010203, 2015.

Cavan, E. L., Henson, S. A., Belcher, A., and Sanders, R.: Role of zooplankton in determining the efficiency of the biological carbon pump, Biogeosciences, 14, 177–186, https://doi.org/10.5194/bg-14-177-2017, 2017.

Charalampopoulou, A., Poulton, A. J., Bakker, D. C. E., Lucas, M. I., Stinchcombe, M. C., and Tyrrell, T.: Environmental drivers of coccolithophore abundance and calcification across Drake Passage (Southern Ocean), Biogeosciences, 13, 5917–5935, https://doi.org/10.5194/bg-13-5917-2016, 2016.

Coggins, A., Watson, A. J., Schuster, U., Mackay, N., King, B., McDonagh, E., and Poulton, A. J.: Surface ocean carbon budget in the 2017 south Georgia diatom bloom: Observations and validation of profiling biogeochemical argo floats, Deep-Sea Res. Pt. II, 209, 105275, https://doi.org/10.1016/j.dsr2.2023.105275, 2023.

Constable, A. J., Melbourne-Thomas, J., Corney, S. P., Arrigo, K. R., Barbraud, C., Barnes, D. K. A., Bindoff, N. L., Boyd, P. W., Brandt, A., Costa, D. P., Davidson, A. T., Ducklow, H. W., Emmerson, L., Fukuchi, M., Gutt, J., Hindell, M. A., Hofmann, E. E., Hosie, G. W., Iida, T., Jacob, S., Johnston, N. M., Kawaguchi, S., Kokubun, N., Koubbi, P., Lea, M.-A., Makhado, A., Massom, R. A., Meiners, K., Meredith, M. P., Murphy, E. J., Nicol, S., Reid, K., Richerson, K., Riddle, M. J., Rintoul, S. R., Smith Jr, W. O., Southwell, C., Stark, J. S., Sumner, M., Swadling, K. M., Takahashi, K. T., Trathan, P. N., Welsford, D. C., Weimerskirch, H., Westwood, K. J., Wienecke, B. C., Wolf-Gladrow, D., Wright, S. W., Xavier, J. C., and Ziegler, P.: Climate change and Southern Ocean ecosystems I: how changes in physical habitats directly affect marine biota, Glob. Change Biol., 20, 3004–3025, https://doi.org/10.1111/gcb.12623, 2014.

Death, R., Wadham, J. L., Monteiro, F., Le Brocq, A. M., Tranter, M., Ridgwell, A., Dutkiewicz, S., and Raiswell, R.: Antarctic ice sheet fertilises the Southern Ocean, Biogeosciences, 11, 2635–2643, https://doi.org/10.5194/bg-11-2635-2014, 2014.

de Baar, H. J. W., de Jong, J. T. M., Bakker, D. C. E., Löscher, B. M., Veth, C., Bathmann, U., and Smetacek, V.: Importance of iron for plankton blooms and carbon dioxide drawdown in the Southern Ocean, Nature, 373, 412–415, https://doi.org/10.1038/373412a0, 1995.

Deppeler, S. L. and Davidson, A. T.: Southern Ocean Phytoplankton in a Changing Climate, Frontiers in Marine Science, 4, 40 https://doi.org/10.3389/fmars.2017.00040, 2017.

DeVries, T.: The oceanic anthropogenic CO_2 sink: Storage, air-sea fluxes, and transports over the industrial era, Global Biogeochem. Cy., 28, 631–647, https://doi.org/10.1002/2013gb004739, 2014.

Ducklow, H. W., Baker, K., Martinson, D. G., Quetin, L. B., Ross, R. M., Smith, R. C., Stammerjohn, S. E., Vernet, M., and Fraser, W.: Marine pelagic ecosystems: the west Antarctic Peninsula, Philos. T. R. Soc. Lon. B, 362, 67–94, https://doi.org/10.1098/rstb.2006.1955, 2007.

ESGF: CMIP6, ESGF [data set], https://esgf-node.llnl.gov/search/cmip6/, last access: 11 February 2025.

Fisher, B. J., Poulton, A. J., Meredith, M. P., Baldry, K., Schofield, O., and Henley, S.: Climate driven shifts in Southern Ocean primary producers and biogeochemistry in CMIP6 models: code, Version 3, Zenodo [code], https://doi.org/10.5281/zenodo.14536775, 2024.

Freeman, N. M., Lovenduski, N. S., Munro, D. R., Krumhardt, K. M., Lindsay, K., Long, M. C., and Maclennan, M.: The Variable and Changing Southern Ocean Silicate Front: Insights From the

CESM Large Ensemble, Global Biogeochem. Cy., 32, 752–768, https://doi.org/10.1029/2017gb005816, 2018.

Friedlingstein, P., Jones, M. W., O'Sullivan, M., Andrew, R. M., Bakker, D. C. E., Hauck, J., Le Quéré, C., Peters, G. P., Peters, W., Pongratz, J., Sitch, S., Canadell, J. G., Ciais, P., Jackson, R. B., Alin, S. R., Anthoni, P., Bates, N. R., Becker, M., Bellouin, N., Bopp, L., Chau, T. T. T., Chevallier, F., Chini, L. P., Cronin, M., Currie, K. I., Decharme, B., Djeutchouang, L. M., Dou, X., Evans, W., Feely, R. A., Feng, L., Gasser, T., Gilfillan, D., Gkritzalis, T., Grassi, G., Gregor, L., Gruber, N., Gürses, Ö., Harris, I., Houghton, R. A., Hurtt, G. C., Iida, Y., Ilyina, T., Luijkx, I. T., Jain, A., Jones, S. D., Kato, E., Kennedy, D., Klein Goldewijk, K., Knauer, J., Korsbakken, J. I., Körtzinger, A., Landschützer, P., Lauvset, S. K., Lefèvre, N., Lienert, S., Liu, J., Marland, G., McGuire, P. C., Melton, J. R., Munro, D. R., Nabel, J. E. M. S., Nakaoka, S.-I., Niwa, Y., Ono, T., Pierrot, D., Poulter, B., Rehder, G., Resplandy, L., Robertson, E., Rödenbeck, C., Rosan, T. M., Schwinger, J., Schwingshackl, C., Séférian, R., Sutton, A. J., Sweeney, C., Tanhua, T., Tans, P. P., Tian, H., Tilbrook, B., Tubiello, F., van der Werf, G. R., Vuichard, N., Wada, C., Wanninkhof, R., Watson, A. J., Willis, D., Wiltshire, A. J., Yuan, W., Yue, C., Yue, X., Zaehle, S., and Zeng, J.: Global Carbon Budget 2021, Earth Syst. Sci. Data, 14, 1917–2005, https://doi.org/10.5194/essd-14-1917-2022, 2022.

Frölicher, T. L., Sarmiento, J. L., Paynter, D. J., Dunne, J. P., Krasting, J. P., and Winton, M.: Dominance of the Southern Ocean in Anthropogenic Carbon and Heat Uptake in CMIP5 Models, J. Climate, 28, 862–886, https://doi.org/10.1175/jcli-d-14-00117.1, 2015.

Fu, W., Randerson, J. T., and Moore, J. K.: Climate change impacts on net primary production (NPP) and export production (EP) regulated by increasing stratification and phytoplankton community structure in the CMIP5 models, Biogeosciences, 13, 5151–5170, https://doi.org/10.5194/bg-13-5151-2016, 2016.

Fu, W., Moore, J. K., Primeau, F., Collier, N., Ogunro, O. O., Hoffman, F. M., and Randerson, J. T.: Evaluation of Ocean Biogeochemistry and Carbon Cycling in CMIP Earth System Models With the International Ocean Model Benchmarking (IOMB) Software System, J. Geophys. Res.-Oceans, 127, e2022JC018965, https://doi.org/10.1029/2022jc018965, 2022.

Garcia, H., Weathers, K., Paver, C., Smolyar, I., Boyer, T., Locarnini, M., Zweng, M., Mishonov, A., Baranova, O., and Seidov, D.: World ocean atlas 2018. Vol. 4: Dissolved inorganic nutrients (phosphate, nitrate and nitrate+ nitrite, silicate), https://data.nodc.noaa.gov/woa/WOA18/DOC/woa18_vol4.pdf (last access: 11 February 2025), 2019.

Gregg, W. W., Conkright, M. E., Ginoux, P., O'Reilly, J. E., and Casey, N. W.: Ocean primary production and climate: Global decadal changes, Geophys. Res. Lett., 30, 1809, https://doi.org/10.1029/2003gl016889, 2003.

Gregor, L., Kok, S., and Monteiro, P. M. S.: Interannual drivers of the seasonal cycle of CO_2 in the Southern Ocean, Biogeosciences, 15, 2361–2378, https://doi.org/10.5194/bg-15-2361-2018, 2018.

Grover, M.: Correctly Calculating Annual Averages with Xarray, https://ncar.github.io/esds/posts/2021/yearly-averages-xarray/ (last access: 11 February 2025), 2021.

Gruber, N., Landschutzer, P., and Lovenduski, N. S.: The Variable Southern Ocean Carbon Sink, Annu. Rev. Mar. Sci., 11, 159–186, https://doi.org/10.1146/annurev-marine-121916-063407, 2019.

Guidi, L., Chaffron, S., Bittner, L., Eveillard, D., Larhlimi, A., Roux, S., Darzi, Y., Audic, S., Berline, L., Brum, J., Coelho, L. P., Espinoza, J. C. I., Malviya, S., Sunagawa, S., Dimier, C., Kandels-Lewis, S., Picheral, M., Poulain, J., Searson, S., Tara Oceans, c., Stemmann, L., Not, F., Hingamp, P., Speich, S., Follows, M., Karp-Boss, L., Boss, E., Ogata, H., Pesant, S., Weissenbach, J., Wincker, P., Acinas, S. G., Bork, P., de Vargas, C., Iudicone, D., Sullivan, M. B., Raes, J., Karsenti, E., Bowler, C., and Gorsky, G.: Plankton networks driving carbon export in the oligotrophic ocean, Nature, 532, 465–470, https://doi.org/10.1038/nature16942, 2016.

Haberman, K. L., Ross, R. M., and Quetin, L. B.: Diet of the Antarctic krill (Euphausia superba Dana): II.: Selective grazing in mixed phytoplankton assemblages, J. Exp. Mar. Biol. Ecol., 283, 97–113, https://doi.org/10.1016/S0022-0981(02)00467-7, 2003.

Hauck, J., Völker, C., Wolf-Gladrow, D. A., Laufkötter, C., Vogt, M., Aumont, O., Bopp, L., Buitenhuis, E. T., Doney, S. C., Dunne, J., Gruber, N., Hashioka, T., John, J., Le Quéré, C., Lima, I. D., Nakano, H., Séférian, R., and Totterdell, I.: On the Southern Ocean CO_2 uptake and the role of the biological carbon pump in the 21st century, Global Biogeochem. Cy., 29, 1451–1470, https://doi.org/10.1002/2015gb005140, 2015.

Heneghan, R. F., Everett, J. D., Blanchard, J. L., Sykes, P., and Richardson, A. J.: Climate-driven zooplankton shifts cause large-scale declines in food quality for fish, Nat. Clim. Change, 13, 470–477, https://doi.org/10.1038/s41558-023-01630-7, 2023.

Henley, S. F., Tuerena, R. E., Annett, A. L., Fallick, A. E., Meredith, M. P., Venables, H. J., Clarke, A., and Ganeshram, R. S.: Macronutrient supply, uptake and recycling in the coastal ocean of the west Antarctic Peninsula, Deep-Sea Res. Pt. II, 139, 58–76, https://doi.org/10.1016/j.dsr2.2016.10.003, 2017.

Henley, S. F., Schofield, O. M., Hendry, K. R., Schloss, I. R., Steinberg, D. K., Moffat, C., Peck, L. S., Costa, D. P., Bakker, D. C. E., Hughes, C., Rozema, P. D., Ducklow, H. W., Abele, D., Stefels, J., Van Leeuwe, M. A., Brussaard, C. P. D., Buma, A. G. J., Kohut, J., Sahade, R., Friedlaender, A. S., Stammerjohn, S. E., Venables, H. J., and Meredith, M. P.: Variability and change in the west Antarctic Peninsula marine system: Research priorities and opportunities, Prog. Oceanogr., 173, 208–237, https://doi.org/10.1016/j.pocean.2019.03.003, 2019.

Henley, S. F., Cavan, E. L., Fawcett, S. E., Kerr, R., Monteiro, T., Sherrell, R. M., Bowie, A. R., Boyd, P. W., Barnes, D. K. A., Schloss, I. R., Marshall, T., Flynn, R., and Smith, S.: Changing Biogeochemistry of the Southern Ocean and Its Ecosystem Implications, Frontiers in Marine Science, 7, 581, https://doi.org/10.3389/fmars.2020.00581, 2020.

Henson, S. A., Cael, B. B., Allen, S. R., and Dutkiewicz, S.: Future phytoplankton diversity in a changing climate, Nat. Commun., 12, 5372, https://doi.org/10.1038/s41467-021-25699-w, 2021.

Henson, S. A., Laufkötter, C., Leung, S., Giering, S. L. C., Palevsky, H. I., and Cavan, E. L.: Uncertain response of ocean biological carbon export in a changing world, Nat. Geosci., 15, 248–254, https://doi.org/10.1038/s41561-022-00927-0, 2022.

Hudson, R. J. and Morel, F. M.: lron transport in marine phytoplankton: Kinetics of cellular and medium coordination reactions, Limnol. Oceanogr., 35, 1002–1020, 1990.

Jabre, L. J., Allen, A. E., McCain, J. S. P., McCrow, J. P., Tenenbaum, N., Spackeen, J. L., Sipler, R. E., Green, B. R., Bronk, D. A., Hutchins, D. A., and Bertrand, E. M.: Molecular underpinnings and biogeochemical consequences of enhanced diatom growth in a warming Southern Ocean, P. Natl. Acad. Sci. USA, 118, e2107238118, https://doi.org/10.1073/pnas.2107238118, 2021.

Jiang, L.-Q., Carter, B. R., Feely, R. A., Lauvset, S. K., and Olsen, A.: Surface ocean pH and buffer capacity: past, present and future, Sci. Rep., 9, 18624, https://doi.org/10.1038/s41598-019-55039-4, 2019.

Jin, X., Gruber, N., Dunne, J. P., Sarmiento, J. L., and Armstrong, R. A.: Diagnosing the contribution of phytoplankton functional groups to the production and export of particulate organic carbon, $CaCO_3$, and opal from global nutrient and alkalinity distributions, Global Biogeochem. Cy., 20, GB2015, https://doi.org/10.1029/2005gb002532, 2006.

Kang, S. H., Kang, J. S., Lee, S., Chung, K. H., Kim, D., and Park, M. G.: Antarctic phytoplankton assemblages in the marginal ice zone of the northwestern Weddell Sea, J. Plankton Res., 23, 333–352, https://doi.org/10.1093/plankt/23.4.333, 2001.

Kawaguchi, S., Ishida, A., King, R., Raymond, B., Waller, N., Constable, A., Nicol, S., Wakita, M., and Ishimatsu, A.: Risk maps for Antarctic krill under projected Southern Ocean acidification, Nat. Clim. Change, 3, 843–847, https://doi.org/10.1038/Nclimate1937, 2013.

Kwiatkowski, L., Aumont, O., Bopp, L., and Ciais, P.: The Impact of Variable Phytoplankton Stoichiometry on Projections of Primary Production, Food Quality, and Carbon Uptake in the Global Ocean, Global Biogeochem. Cy., 32, 516–528, https://doi.org/10.1002/2017gb005799, 2018.

Kwon, E. Y., Sreeush, M. G., Timmermann, A., Karl, D. M., Church, M. J., Lee, S.-S., and Yamaguchi, R.: Nutrient uptake plasticity in phytoplankton sustains future ocean net primary production, Science Advances, 8, eadd2475, https://doi.org/10.1126/sciadv.add2475, 2022.

Landschutzer, P., Gruber, N., Haumann, F. A., Rodenbeck, C., Bakker, D. C., van Heuven, S., Hoppema, M., Metzl, N., Sweeney, C., Takahashi, T., Tilbrook, B., and Wanninkhof, R.: The reinvigoration of the Southern Ocean carbon sink, Science, 349, 1221–1224, https://doi.org/10.1126/science.aab2620, 2015.

Lannuzel, D., Chever, F., van der Merwe, P. C., Janssens, J., Roukaerts, A., Cavagna, A. J., Townsend, A. T., Bowie, A. R., and Meiners, K. M.: Iron biogeochemistry in Antarctic pack ice during SIPEX-2, Deep-Sea Res. Pt. II, 131, 111–122, https://doi.org/10.1016/j.dsr2.2014.12.003, 2016.

Laufkötter, C., Vogt, M., Gruber, N., Aita-Noguchi, M., Aumont, O., Bopp, L., Buitenhuis, E., Doney, S. C., Dunne, J., Hashioka, T., Hauck, J., Hirata, T., John, J., Le Quéré, C., Lima, I. D., Nakano, H., Seferian, R., Totterdell, I., Vichi, M., and Völker, C.: Drivers and uncertainties of future global marine primary production in marine ecosystem models, Biogeosciences, 12, 6955–6984, https://doi.org/10.5194/bg-12-6955-2015, 2015.

Leung, S., Cabré, A., and Marinov, I.: A latitudinally banded phytoplankton response to 21st century climate change in the Southern Ocean across the CMIP5 model suite, Biogeosciences, 12, 5715–5734, https://doi.org/10.5194/bg-12-5715-2015, 2015.

Lewandowska, A. M., Hillebrand, H., Lengfellner, K., and Sommer, U.: Temperature effects on phytoplankton diversity - The zooplankton link, J. Sea Res., 85, 359–364, https://doi.org/10.1016/j.seares.2013.07.003, 2014.

Litchman, E. and Klausmeier, C. A.: Trait-Based Community Ecology of Phytoplankton, Annu. Rev. Ecol. Evol. S., 39, 615–639, https://doi.org/10.1146/annurev.ecolsys.39.110707.173549, 2008.

Llort, J., Lévy, M., Sallée, J. B., and Tagliabue, A.: Nonmonotonic Response of Primary Production and Export to Changes in Mixed-Layer Depth in the Southern Ocean, Geophys. Res. Lett., 46, 3368–3377, https://doi.org/10.1029/2018gl081788, 2019.

Long, M. C., Moore, J. K., Lindsay, K., Levy, M., Doney, S. C., Luo, J. Y., Krumhardt, K. M., Letscher, R. T., Grover, M., and Sylvester, Z. T.: Simulations With the Marine Biogeochemistry Library (MARBL), J. Adv. Model. Earth Sy., 13, e2021MS002647, https://doi.org/10.1029/2021MS002647, 2021.

Lopez-Urrutia, A., San Martin, E., Harris, R. P., and Irigoien, X.: Scaling the metabolic balance of the oceans, P. Natl. Acad. Sci. USA, 103, 8739–8744, https://doi.org/10.1073/pnas.0601137103, 2006.

Luo, Y.-W., Doney, S. C., Anderson, L. A., Benavides, M., Berman-Frank, I., Bode, A., Bonnet, S., Boström, K. H., Böttjer, D., Capone, D. G., Carpenter, E. J., Chen, Y. L., Church, M. J., Dore, J. E., Falcón, L. I., Fernández, A., Foster, R. A., Furuya, K., Gómez, F., Gundersen, K., Hynes, A. M., Karl, D. M., Kitajima, S., Langlois, R. J., LaRoche, J., Letelier, R. M., Marañón, E., McGillicuddy Jr., D. J., Moisander, P. H., Moore, C. M., Mouriño-Carballido, B., Mulholland, M. R., Needoba, J. A., Orcutt, K. M., Poulton, A. J., Rahav, E., Raimbault, P., Rees, A. P., Riemann, L., Shiozaki, T., Subramaniam, A., Tyrrell, T., Turk-Kubo, K. A., Varela, M., Villareal, T. A., Webb, E. A., White, A. E., Wu, J., and Zehr, J. P.: Database of diazotrophs in global ocean: abundance, biomass and nitrogen fixation rates, Earth Syst. Sci. Data, 4, 47–73, https://doi.org/10.5194/essd-4-47-2012, 2012.

Mascioni, M., Almandoz, G. O., Cefarelli, A. O., Cusick, A., Ferrario, M. E., and Vernet, M.: Phytoplankton composition and bloom formation in unexplored nearshore waters of the western Antarctic Peninsula, Polar Biol., 42, 1859–1872, https://doi.org/10.1007/s00300-019-02564-7, 2019.

Masson-Delmotte, V., Zhai, P., Pirani, A., Connors, S. L., Péan, C., Berger, S., Caud, N., Chen, Y., Goldfarb, L., and Gomis, M.: Climate change 2021: the physical science basis, Contribution of working group I to the sixth assessment report of the intergovernmental panel on climate change, 2, https://doi.org/10.1017/9781009157896, 2021.

Matsuoka, K., Skoglund, A., Roth, G., de Pomereu, J., Griffiths, H., Headland, R., Herried, B., Katsumata, K., Le Brocq, A., Licht, K., Morgan, F., Neff, P. D., Ritz, C., Scheinert, M., Tamura, T., Van de Putte, A., van den Broeke, M., von Deschwanden, A., Deschamps-Berger, C., Van Liefferinge, B., Tronstad, S., and Melvær, Y.: Quantarctica, an integrated mapping environment for Antarctica, the Southern Ocean, and sub-Antarctic islands, Environ. Modell. Softw., 140, 105015, https://doi.org/10.1016/j.envsoft.2021.105015, 2021.

Mayzaud, P. and Pakhomov, E. A.: The role of zooplankton communities in carbon recycling in the Ocean: the case of the Southern Ocean, J. Plankton Res., 36, 1543–1556, https://doi.org/10.1093/plankt/fbu076, 2014.

Mendes, C. R. B., Costa, R. R., Ferreira, A., Jesus, B., Tavano, V. M., Dotto, T. S., Leal, M. C., Kerr, R., Islabao, C. A., Franco, A., Mata, M. M., Garcia, C. A. E., and Secchi, E. R.: Cryptophytes: An emerging algal group in the rapidly changing Antarctic Peninsula marine environments, Glob. Change Biol., 29, 1791–1808, https://doi.org/10.1111/gcb.16602, 2023.

Meredith, M., Sommerkorn, M., Cassotta, S., Derksen, C., Ekaykin, A., Hollowed, A., Kofinas, G., Mackintosh, A., Melbourne-Thomas, J., and Muelbert, M.: Chapter 3: polar regions, IPCC special report on the ocean and cryosphere in a changing climate, 5, https://www.ipcc.ch/site/assets/uploads/sites/3/2019/11/07_SROCC_Ch03_FINAL.pdf (last access: 11 February 2025), 2019.

Moline, M. A., Claustre, H., Frazer, T. K., Schofield, O., and Vernet, M.: Alteration of the food web along the Antarctic Peninsula in response to a regional warming trend, Glob. Change Biol., 10, 1973–1980, https://doi.org/10.1111/j.1365-2486.2004.00825.x, 2004.

Moline, M. A., Karnovsky, N. J., Brown, Z., Divoky, G. J., Frazer, T. K., Jacoby, C. A., Torrese, J. J., and Fraser, W. R.: High latitude changes in ice dynamics and their impact on polar marine ecosystems, Ann. NY Acad. Sci., 1134, 267–319, https://doi.org/10.1196/annals.1439.010, 2008.

Montes-Hugo, M. A., Vernet, M., Martinson, D., Smith, R., and Iannuzzi, R.: Variability on phytoplankton size structure in the western Antarctic Peninsula (1997–2006), Deep-Sea Res. Pt. II, 55, 2106–2117, https://doi.org/10.1016/j.dsr2.2008.04.036, 2008.

Moore, C. M., Mills, M. M., Arrigo, K. R., Berman-Frank, I., Bopp, L., Boyd, P. W., Galbraith, E. D., Geider, R. J., Guieu, C., Jaccard, S. L., Jickells, T. D., La Roche, J., Lenton, T. M., Mahowald, N. M., Marañón, E., Marinov, I., Moore, J. K., Nakatsuka, T., Oschlies, A., Saito, M. A., Thingstad, T. F., Tsuda, A., and Ulloa, O.: Processes and patterns of oceanic nutrient limitation, Nat. Geosci., 6, 701–710, https://doi.org/10.1038/Ngeo1765, 2013.

Moore, J. K., Doney, S. C., and Lindsay, K.: Upper ocean ecosystem dynamics and iron cycling in a global three-dimensional model, Global Biogeochem. Cy., 18, GB4028, https://doi.org/10.1029/2004gb002220, 2004.

Moreau, S., Mostajir, B., Belanger, S., Schloss, I. R., Vancoppenolle, M., Demers, S., and Ferreyra, G. A.: Climate change enhances primary production in the western Antarctic Peninsula, Glob. Change Biol., 21, 2191–2205, https://doi.org/10.1111/gcb.12878, 2015.

Moreau, S., Boyd, P. W., and Strutton, P. G.: Remote assessment of the fate of phytoplankton in the Southern Ocean sea-ice zone, Nat. Commun., 11, 3108, https://doi.org/10.1038/s41467-020-16931-0, 2020.

Moreau, S., Hattermann, T., de Steur, L., Kauko, H. M., Ahonen, H., Ardelan, M., Assmy, P., Chierici, M., Descamps, S., Dinter, T., Falkenhaug, T., Fransson, A., Gronningsaeter, E., Hallfredsson, E. H., Huhn, O., Lebrun, A., Lowther, A., Lubcker, N., Monteiro, P., Peeken, I., Roychoudhury, A., Rozanska, M., Ryan-Keogh, T., Sanchez, N., Singh, A., Simonsen, J. H., Steiger, N., Thomalla, S. J., van Tonder, A., Wiktor, J. M., and Steen, H.: Wind-driven upwelling of iron sustains dense blooms and food webs in the eastern Weddell Gyre, Nat. Commun., 14, 1303, https://doi.org/10.1038/s41467-023-36992-1, 2023.

Nissen, C., Vogt, M., Münnich, M., Gruber, N., and Haumann, F. A.: Factors controlling coccolithophore biogeography in the Southern Ocean, Biogeosciences, 15, 6997–7024, https://doi.org/10.5194/bg-15-6997-2018, 2018.

O'Neill, B. C., Tebaldi, C., van Vuuren, D. P., Eyring, V., Friedlingstein, P., Hurtt, G., Knutti, R., Kriegler, E., Lamarque, J.-F., Lowe, J., Meehl, G. A., Moss, R., Riahi, K., and Sanderson, B. M.: The Scenario Model Intercomparison Project (ScenarioMIP) for CMIP6, Geosci. Model Dev., 9, 3461–3482, https://doi.org/10.5194/gmd-9-3461-2016, 2016.

Pausch, F., Bischof, K., and Trimborn, S.: Iron and manganese co-limit growth of the Southern Ocean diatom Chaetoceros debilis, PLoS One, 14, e0221959, https://doi.org/10.1371/journal.pone.0221959, 2019.

Pearce, I., Davidson, A. T., Thomson, P. G., Wright, S., and van den Enden, R.: Marine microbial ecology in the sub-Antarctic Zone: Rates of bacterial and phytoplankton growth and grazing by heterotrophic protists, Deep-Sea Res. Pt. II, 58, 2248–2259, https://doi.org/10.1016/j.dsr2.2011.05.030, 2011.

Person, R., Aumont, O., and Lévy, M.: The Biological Pump and Seasonal Variability of pCO_2 in the Southern Ocean: Exploring the Role of Diatom Adaptation to Low Iron, J. Geophys. Res.-Oceans, 123, 3204–3226, https://doi.org/10.1029/2018jc013775, 2018.

Petrou, K., Baker, K. G., Nielsen, D. A., Hancock, A. M., Schulz, K. G., and Davidson, A. T.: Acidification diminishes diatom silica production in the Southern Ocean, Nat. Clim. Change, 9, 781–786, https://doi.org/10.1038/s41558-019-0557-y, 2019.

Purich, A. and England, M. H.: Historical and Future Projected Warming of Antarctic Shelf Bottom Water in CMIP6 Models, Geophys. Res. Lett., 48, e2021GL092752, https://doi.org/10.1029/2021GL092752, 2021.

Quéguiner, B.: Iron fertilization and the structure of planktonic communities in high nutrient regions of the Southern Ocean, Deep-Sea Res. Pt. II, 90, 43–54, https://doi.org/10.1016/j.dsr2.2012.07.024, 2013.

Raphael, M. N. and Handcock, M. S.: A new record minimum for Antarctic sea ice, Nature Reviews Earth & Environment, 3, 215–216, https://doi.org/10.1038/s43017-022-00281-0, 2022.

Ratnarajah, L., Abu-Alhaija, R., Atkinson, A., Batten, S., Bax, N. J., Bernard, K. S., Canonico, G., Cornils, A., Everett, J. D., Grigoratou, M., Ishak, N. H. A., Johns, D., Lombard, F., Muxagata, E., Ostle, C., Pitois, S., Richardson, A. J., Schmidt, K., Stemmann, L., Swadling, K. M., Yang, G., and Yebra, L.: Monitoring and modelling marine zooplankton in a changing climate, Nat. Commun., 14, 564, https://doi.org/10.1038/s41467-023-36241-5, 2023.

Riebesell, U., Schulz, K. G., Bellerby, R. G., Botros, M., Fritsche, P., Meyerhofer, M., Neill, C., Nondal, G., Oschlies, A., Wohlers, J., and Zollner, E.: Enhanced biological carbon consumption in a high CO_2 ocean, Nature, 450, 545–548, https://doi.org/10.1038/nature06267, 2007.

Roach, L. A., Dörr, J., Holmes, C. R., Massonnet, F., Blockley, E. W., Notz, D., Rackow, T., Raphael, M. N., O'Farrell, S. P., Bailey, D. A., and Bitz, C. M.: Antarctic Sea Ice Area in CMIP6, Geophys. Res. Lett., 47, e2019GL086729, https://doi.org/10.1029/2019GL086729, 2020.

Robinson, J., Popova, E. E., Srokosz, M. A., and Yool, A.: A tale of three islands: Downstream natural iron fertilization in

the Southern Ocean, J. Geophys. Res.-Oceans, 121, 3350–3371, https://doi.org/10.1002/2015JC011319, 2016.

Rohr, T., Richardson, A. J., Lenton, A., Chamberlain, M. A., and Shadwick, E. H.: Zooplankton grazing is the largest source of uncertainty for marine carbon cycling in CMIP6 models, Communications Earth & Environment, 4, 212, https://doi.org/10.1038/s43247-023-00871-w, 2023.

Rozema, P. D., Venables, H. J., van de Poll, W. H., Clarke, A., Meredith, M. P., and Buma, A. G. J.: Interannual variability in phytoplankton biomass and species composition in northern Marguerite Bay (West Antarctic Peninsula) is governed by both winter sea ice cover and summer stratification, Limnol. Oceanogr., 62, 235–252, https://doi.org/10.1002/lno.10391, 2017.

Saba, G. K., Fraser, W. R., Saba, V. S., Iannuzzi, R. A., Coleman, K. E., Doney, S. C., Ducklow, H. W., Martinson, D. G., Miles, T. N., Patterson-Fraser, D. L., Stammerjohn, S. E., Steinberg, D. K., and Schofield, O. M.: Winter and spring controls on the summer food web of the coastal West Antarctic Peninsula, Nat. Commun., 5, 4318, https://doi.org/10.1038/ncomms5318, 2014.

Sallee, J. B., Pellichero, V., Akhoudas, C., Pauthenet, E., Vignes, L., Schmidtko, S., Garabato, A. N., Sutherland, P., and Kuusela, M.: Summertime increases in upper-ocean stratification and mixed-layer depth, Nature, 591, 592–598, https://doi.org/10.1038/s41586-021-03303-x, 2021.

Sarmiento, J. L., Gruber, N., Brzezinski, M. A., and Dunne, J. P.: High-latitude controls of thermocline nutrients and low latitude biological productivity, Nature, 427, 56–60, https://doi.org/10.1038/nature02127, 2004.

Sathyendranath, S., Stuart, V., Nair, A., Oka, K., Nakane, T., Bouman, H., Forget, M. H., Maass, H., and Platt, T.: Carbon-to-chlorophyll ratio and growth rate of phytoplankton in the sea, Mar. Ecol. Prog. Ser., 383, 73–84, https://doi.org/10.3354/meps07998, 2009.

Schofield, O., Brown, M., Kohut, J., Nardelli, S., Saba, G., Waite, N., and Ducklow, H.: Changes in the upper ocean mixed layer and phytoplankton productivity along the West Antarctic Peninsula, Philos. T. Roy. Soc. A, 376, 20170173, https://doi.org/10.1098/rsta.2017.0173, 2018.

Seferian, R., Berthet, S., Yool, A., Palmieri, J., Bopp, L., Tagliabue, A., Kwiatkowski, L., Aumont, O., Christian, J., Dunne, J., Gehlen, M., Ilyina, T., John, J. G., Li, H., Long, M. C., Luo, J. Y., Nakano, H., Romanou, A., Schwinger, J., Stock, C., Santana-Falcon, Y., Takano, Y., Tjiputra, J., Tsujino, H., Watanabe, M., Wu, T., Wu, F., and Yamamoto, A.: Tracking Improvement in Simulated Marine Biogeochemistry Between CMIP5 and CMIP6, Curr. Clim. Change Rep., 6, 95–119, https://doi.org/10.1007/s40641-020-00160-0, 2020.

Shu, Q., Wang, Q., Song, Z. Y., Qiao, F. L., Zhao, J. C., Chu, M., and Li, X. F.: Assessment of Sea Ice Extent in CMIP6 With Comparison to Observations and CMIP5, Geophys. Res. Lett., 47, e2020GL087965, https://doi.org/10.1029/2020GL087965, 2020.

Steiner, N. S., Bowman, J., Campbell, K., Chierici, M., Eronen-Rasimus, E., Falardeau, M., Flores, H., Fransson, A., Herr, H., and Insley, S. J.: Climate change impacts on sea-ice ecosystems and associated ecosystem services, Elem. Sci. Anth., 9, 00007, https://doi.org/10.1525/elementa.2021.00007, 2021.

Stock, C. A., Dunne, J. P., and John, J. G.: Global-scale carbon and energy flows through the marine planktonic food web: An analysis with a coupled physical–biological model, Prog. Oceanogr., 120, 1–28, https://doi.org/10.1016/j.pocean.2013.07.001, 2014.

Stock, C. A., Dunne, J. P., Fan, S. M., Ginoux, P., John, J., Krasting, J. P., Laufkötter, C., Paulot, F., and Zadeh, N.: Ocean Biogeochemistry in GFDL's Earth System Model 4.1 and Its Response to Increasing Atmospheric CO_2, J. Adv. Model. Earth Sy., 12, e2019MS002043, https://doi.org/10.1029/2019MS002043, 2020.

Strzepek, R. F. and Harrison, P. J.: Photosynthetic architecture differs in coastal and oceanic diatoms, Nature, 431, 689–692, https://doi.org/10.1038/nature02954, 2004.

Sunagawa, S., Acinas, S. G., Bork, P., Bowler, C., Tara Oceans, C., Eveillard, D., Gorsky, G., Guidi, L., Iudicone, D., Karsenti, E., Lombard, F., Ogata, H., Pesant, S., Sullivan, M. B., Wincker, P., and de Vargas, C.: Tara Oceans: towards global ocean ecosystems biology, Nat. Rev. Microbiol., 18, 428–445, https://doi.org/10.1038/s41579-020-0364-5, 2020.

Swadling, K. M., Constable, A. J., Fraser, A. D., Massom, R. A., Borup, M. D., Ghigliotti, L., Granata, A., Guglielmo, L., Johnston, N. M., Kawaguchi, S., Kennedy, F., Kiko, R., Koubbi, P., Makabe, R., Martin, A., McMinn, A., Moteki, M., Pakhomov, E. A., Peeken, I., Reimer, J., Reid, P., Ryan, K. G., Vacchi, M., Virtue, P., Weldrick, C. K., Wongpan, P., and Wotherspoon, S. J.: Biological responses to change in Antarctic sea ice habitats, Frontiers in Ecology and Evolution, 10, 1073823, https://doi.org/10.3389/fevo.2022.1073823, 2023.

Tagliabue, A., Aumont, O., DeAth, R., Dunne, J. P., Dutkiewicz, S., Galbraith, E., Misumi, K., Moore, J. K., Ridgwell, A., Sherman, E., Stock, C., Vichi, M., Völker, C., and Yool, A.: How well do global ocean biogeochemistry models simulate dissolved iron distributions?, Global Biogeochem. Cy., 30, 149–174, https://doi.org/10.1002/2015gb005289, 2016.

Tagliabue, A., Kwiatkowski, L., Bopp, L., Butenschön, M., Cheung, W., Lengaigne, M., and Vialard, J.: Persistent Uncertainties in Ocean Net Primary Production Climate Change Projections at Regional Scales Raise Challenges for Assessing Impacts on Ecosystem Services, Frontiers in Climate, 3, 738224, https://doi.org/10.3389/fclim.2021.738224, 2021.

Timmermans, K. R., van der Wagt, B., and de Baar, H. J. W.: Growth rates, half-saturation constants, and silicate, nitrate, and phosphate depletion in relation to iron availability of four large, open-ocean diatoms from the Southern Ocean, Limnol. Oceanogr., 49, 2141–2151, https://doi.org/10.4319/lo.2004.49.6.2141, 2004.

Tortell, P. D., Payne, C. D., Li, Y., Trimborn, S., Rost, B., Smith, W. O., Riesselman, C., Dunbar, R. B., Sedwick, P., and DiTullio, G. R.: CO_2 sensitivity of Southern Ocean phytoplankton, Geophys. Res. Lett., 35, L04605, https://doi.org/10.1029/2007gl032583, 2008.

Touzé-Peiffer, L., Barberousse, A., and Le Treut, H.: The Coupled Model Intercomparison Project: History, uses, and structural effects on climate research, WIRES Clim. Change, 11, e648, https://doi.org/10.1002/wcc.648, 2020.

Tréguer, P., Bowler, C., Moriceau, B., Dutkiewicz, S., Gehlen, M., Aumont, O., Bittner, L., Dugdale, R., Finkel, Z., Iudicone, D., Jahn, O., Guidi, L., Lasbleiz, M., Leblanc, K., Levy, M., and Pondaven, P.: Influence of diatom diversity on the ocean biological carbon pump, Nat. Geosci., 11, 27–37, https://doi.org/10.1038/s41561-017-0028-x, 2017.

Turner, J. and Comiso, J.: Solve Antarctica's sea-ice puzzle, Nature, 547, 275–277, https://doi.org/10.1038/547275a, 2017.

Turner, J., Holmes, C., Harrison, T. C., Phillips, T., Jena, B., Reeves-Francois, T., Fogt, R., Thomas, E. R., and Bajish, C. C.: Record Low Antarctic Sea Ice Cover in February 2022, Geophys. Res. Lett., 49, e2022GL098904, https://doi.org/10.1029/2022GL098904, 2022.

Venables, H. J., Clarke, A., and Meredith, M. P.: Wintertime controls on summer stratification and productivity at the western Antarctic Peninsula, Limnol. Oceanogr., 58, 1035–1047, https://doi.org/10.4319/lo.2013.58.3.1035, 2013.

Virtanen, P., Gommers, R., Oliphant, T. E., Haberland, M., Reddy, T., Cournapeau, D., Burovski, E., Peterson, P., Weckesser, W., and Bright, J.: SciPy 1.0: fundamental algorithms for scientific computing in Python, Nat. Methods, 17, 261–272, 2020.

Ward, B. A. and Follows, M. J.: Marine mixotrophy increases trophic transfer efficiency, mean organism size, and vertical carbon flux, P. Natl. Acad. Sci. USA, 113, 2958–2963, https://doi.org/10.1073/pnas.1517118113, 2016.

Watson, A. J., Bakker, D. C., Ridgwell, A. J., Boyd, P. W., and Law, C. S.: Effect of iron supply on Southern Ocean CO_2 uptake and implications for glacial atmospheric CO_2, Nature, 407, 730–733, https://doi.org/10.1038/35037561, 2000.

Wright, S. W., van den Enden, R. L., Pearce, I., Davidson, A. T., Scott, F. J., and Westwood, K. J.: Phytoplankton community structure and stocks in the Southern Ocean (30–80 E) determined by CHEMTAX analysis of HPLC pigment signatures, Deep-Sea Res. Pt. II, 57, 758–778, 2010.

Xu, K., Fu, F. X., and Hutchins, D. A.: Comparative responses of two dominant Antarctic phytoplankton taxa to interactions between ocean acidification, warming, irradiance, and iron availability, Limnol. Oceanogr., 59, 1919–1931, https://doi.org/10.4319/lo.2014.59.6.1919, 2014.

Zhu, Z., Xu, K., Fu, F. X., Spackeen, J. L., Bronk, D. A., and Hutchins, D. A.: A comparative study of iron and temperature interactive effects on diatoms and Phaeocystis antarctica from the Ross Sea, Antarctica, Mar. Ecol. Prog. Ser., 550, 39–51, https://doi.org/10.3354/meps11732, 2016.

Zhuang, J., Dussin, R., Jüling, A., and Rasp, S.: JiaweiZhuang/xESMF: v0.3.0 Adding ESMF.LocStream capabilities, v0.3.0, Zenodo [code], https://doi.org/10.5281/zenodo.1134365, 2018.